JAERI-Research
2000-051

ULTRAFAST, ULTRAHIGH-PEAK POWER Ti : SAPPHIRE LASER SYSTEM

January 2001

Koichi YAMAKAWA, Makoto AOYAMA,
Shinichi MATSUOKA, Yutaka AKAHANE, Teiji KASE*,
Fumihiko NAKANO and Akito SAGISAKA

日本原子力研究所
Japan Atomic Energy Research Institute

本レポートは，日本原子力研究所が不定期に公刊している研究報告書です。
入手の問合わせは，日本原子力研究所研究情報部研究情報課（〒319-1195　茨城県那珂郡東海村）あて，お申し越しください。なお，このほかに財団法人原子力弘済会資料センター（〒319-1195　茨城県那珂郡東海村日本原子力研究所内）で複写による実費頒布をおこなっております。

This report is issued irregularly.
Inquiries about availability of the reports should be addressed to Research Information Division, Department of Intellectual Resources, Japan Atomic Energy Research Institute, Tokai-mura, Naka-gun, Ibaraki-ken, 319-1195, Japan.

編集兼発行　　日本原子力研究所

JAERI-Research 2000-051

Ultrafast, Ultrahigh-Peak Power Ti:Sapphire Laser System

Koichi YAMAKAWA, Makoto AOYAMA, Shinichi MATSUOKA, Yutaka AKAHANE,
Teiji KASE*, Fumihiko NAKANO and Akito SAGISAKA

Advanced Photon Research Center
Kansai Research Establishment
Japan Atomic Energy Research Institute
Kizu-cho, Souraku-gun, Kyoto

(Received September 22, 2000)

We review progress in the generation of multiterawatt optical pulses in the 10-fs range. We describe a design, performance and characterization of a Ti:sapphire laser system based on chirped-pulse amplification, which has produced a peak power in excess of 100-TW with sub-20-fs pulse durations and an average power of 19-W at a 10-Hz repetition rate. We also discuss extension of this system to the petawatt power level and potential applications in the relativistic, ultrahigh intensity regimes.

Keywords: High Intensity, Laser Amplifiers, Ultrafast Optics, Dispersion Control, Optical Pulse Shaping, Gain Control, Optical Pulse Compression, Solid-State Lasers

---

* on leave from NEC Corporation

極短パルス・超高ピーク出力チタンサファイアレーザー

日本原子力研究所関西研究所光量子科学研究センター
山川 考一・青山 誠・松岡 伸一・赤羽 温
加瀬 貞二*・中野 文彦・匂坂 明人

(２０００年９月２２日受理)

ピーク出力１００テラワット、パルス幅１９フェムト秒、繰り返し１０Ｈｚで動作するチタンサファイアチャープパルスレーザーシステムの設計、性能、特性評価を中心にして、近年の１０フェムト秒領域でのマルチテラワット光パルス発生の進展について紹介する。また、本システムのペタワットレベルへの出力増強の可能性と、このようなレーザーによって生成される超高強度場におけるいくつかの応用研究について議論する。

関西研究所：〒619-0215 京都府相楽郡木津町梅美台8-1
*日本電気株式会社

Contents

目次

1. INTRODUCTION

Recent advances in femtosecond laser sources are making intensities approaching ~ 10^{21} W/cm^2 available for the study of nonlinear relativistic optics [1, 2]. At such intensities the electron velocity in the laser field becomes relativistic and exhibits highly nonlinear motion, thus making it possible to investigate entirely new classes of physical effects. Potential applications of these lasers include the generation of ultrafast x-ray radiation [3-7], ultrahigh-order harmonic generation [8-18], photo-ionization pumped x-ray lasers [19, 20], optical field ionization x-ray lasers [21-24], laser wakefield particle acceleration [25-29], laser induced nuclear photophysics [30, 31], laboratory-based astrophysics [32, 33] and fast ignitor fusion [34, 35].

The technique of chirped pulse amplification (CPA) has opened new avenues for the production of very high-energy ultrashort duration pulses without optical damage to amplifiers and optical components [36, 37]. The combination of CPA and ultrabroad-band solid-state laser materials has made it possible to produce terawatt and even multiterawatt femtosecond pulses with ever increasing average powers [38-41]. The CPA technique consists of four basic components: (1) a short pulse oscillator, (2) a pulse expander, (3) an amplifier, and (4) a pulse compressor. In ultrafast CPA, a short pulse is generated by a mode-locked laser oscillator and is temporally stretched by an antiparallel grating pair pulse expander [42]. The low energy and long duration chirped pulse is then amplified to a high energy commensurate with the saturation fluence of the solid state laser amplifiers. The amplified pulse is then compressed to a transform-limited short pulse of high peak power with a parallel grating pair compressor [43].

Over the past 12 years, peak powers from terawatt CPA systems have steadily increased from less than a terawatt initially to a present record of 1500-TW (1.5-PW). At the same time, pulse durations have steadily decreased from greater than a picosecond to a current record 16-fs [44]. Extremely modest amounts of energy can now be used to achieve multiterawatt peak powers. At the 20-fs pulse duration, for example, only ~ 20-mJ of energy is required to achieve a peak power of 1-TW. Because much less energy is required to reach the same peak power, the size of the laser system can be significantly reduced and the repetition rate of the system can be very high. For instance, the size of the inertial-confinement-fusion Nd:glass laser system such as the NOVA laser at the Lawrence Livermore National Laboratory (LLNL) requires a 200 meter long building to produce 100-TW peak powers in 1-ns duration and the system cannot be operated at more than 1 shot per hour. On the other hand, our 100-TW Ti:sapphire laser system occupies an area of only ~ 15-m^2 and produces the same peak power at 10 shots per second. This capability is especially significant because it allows reliable, high repetition rate, ultrahigh

peak power lasers to become realistic laboratory tools for investigations requiring ultrahigh intensities. In addition the high average power is also desired to produce high fluxes of energetic particles or x-rays and to allow signal averaging techniques to be applied to relativistic laser/matter investigations.

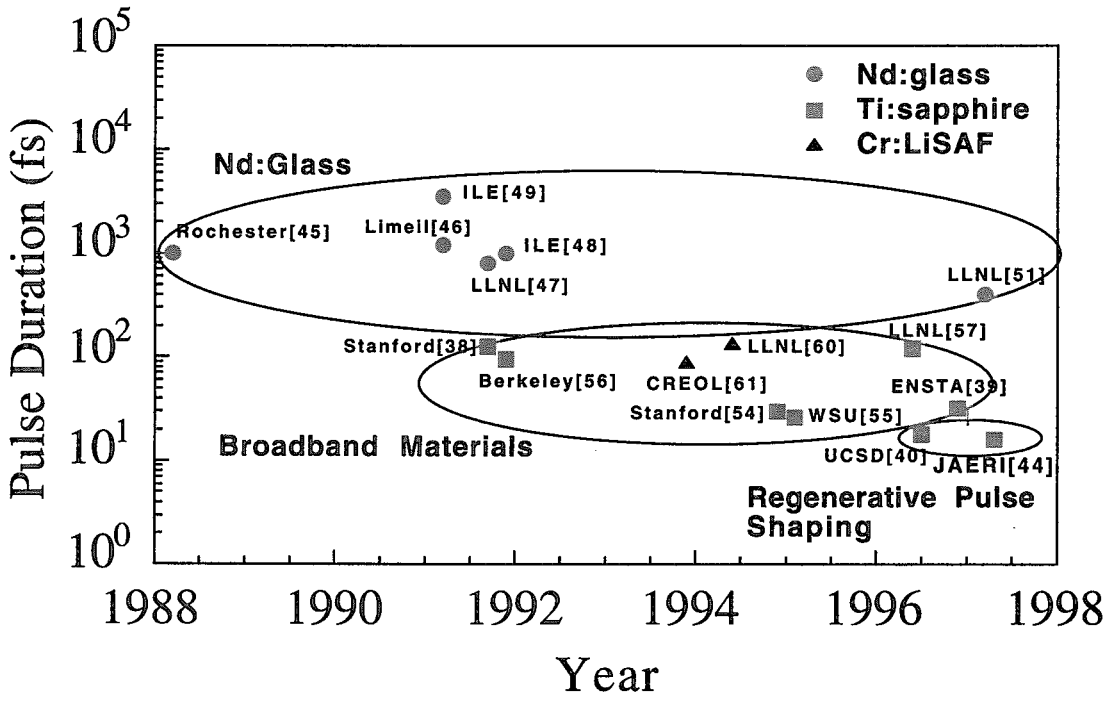

Fig. 1 Representative history of the evolution of terawatt CPA pulse duration.

In this paper we review the evolution of CPA into the 10-fs range. As an example, the design, performance and characterization of a compact three-stage Ti:sapphire CPA laser system at the Japan Atomic Energy Research Institute is described. This system is designed to produce sub-20-fs pulses with peak and average powers of 100-TW and 20-W, respectively at a 10-Hz repetition rate. We also discuss extension of this system to the petawatt power level and potential applications in the nonlinear relativistic intensity regimes.

2. ULTRAFAST CPA TECHNIQUES

The progression of the CPA systems with respect to pulse duration, is illustrated in Fig. 1. The CPA technique has been demonstrated with a variety of laser materials such as

Nd:glass [45-51], alexandrite [52, 53], Ti:sapphire (Ti:Al_2O_3) [38-41, 54-59] and Cr:LiSAlF [60, 61]. These materials all have relatively large saturation fluences of the order of joules per square centimeter, relatively long upper state lifetimes and broad bandwidths. While the first generation of CPA systems were based on Nd:glass amplifiers and generated high energy picosecond pulses, the relatively narrow bandwidth of Nd:glass has limited amplified pulse duration to a few 100's of femtoseconds. To date, pulses as short as 450-fs with over a petawatt peak power have been generated by using a large scale, single-shot-per-hour, inertial-confinement-fusion, Nd:glass laser [62]. While Nd:glass amplifiers have good energy storage and can easily be scaled to large volumes, they are in general limited to low repetition rates and low average power operation because of the poor thermal characteristics of laser glasses. Nevertheless, a terawatt laser with a repetition rate of 1-Hz has been built using a flashlamp-pumped Nd:glass slab power amplifier [63].

Using larger gain bandwidth materials such as Ti:sapphire [64] and Cr:LiSAF [65], however, permits the amplification of sub-100 femtosecond pulses from the Kerr-lens mode-locked oscillators [66-72]. In particular, Ti:sapphire has several desirable characteristics including a high saturation fluences (~ 0.9-J/cm^2), a high thermal conductivity (46-W/mK at 300 K) and a high damage threshold (> 5-J/cm^2) for producing high-peak and high-average power pulses. Its gain bandwidth of ~ 230-nm FWHM could in principle support transform limited pulses of ~ 3-fs. Recently pulses shorter than two optical cycles have been generated directly from Kerr-lens mode-locked Ti:sapphire oscillators by using prism pairs and double chirped mirrors in combination with and without a semiconductor saturable absorber mirror [73, 74]. As for the amplification system, Sartania et al. have demonstrated the generation of 5-fs, 0.5-mJ pulses at a 1-kHz repetition rate using the technique of hollow fiber based pulse compression and ultrabroadband chirped mirrors [75]. Although Ti:sapphire amplifier systems for the generation of pulses with duration of around 20-fs have been demonstrated [76, 77], the amplification of 20-fs pulses to energies greater than one joule has only recently been accomplished [41, 59]. The difficulty lies in the control of two major effects: high-order phase distortion in the amplification chain and gain narrowing in the amplifying media.

To obtain near transform limited pulses through the CPA chain, the phase (group delay) of the pulse must be nearly constant over the broad bandwidth. We can expand the spectral phase $\phi(\omega)$ in a Taylor series about the carrier frequency ω_0:

$$\phi(\omega) = \phi(\omega_0) + \left.\frac{\partial\phi}{\partial\omega}\right|_{\omega_0}(\omega-\omega_0) + \left.\frac{1}{2!}\frac{\partial^2\phi}{\partial\omega^2}\right|_{\omega_0}(\omega-\omega_0)^2$$

$$+\left.\frac{1}{3!}\frac{\partial^3\phi}{\partial\omega^3}\right|_{\omega_0}(\omega-\omega_0)^3 + \left.\frac{1}{4!}\frac{\partial^4\phi}{\partial\omega^4}\right|_{\omega_0}(\omega-\omega_0)^4 + \ldots,$$

(1)

The coefficient of the third term is the second-order–dispersion. The coefficients of the fourth and fifth terms are third- and fourth-order–dispersions, respectively. Terawatt level pulses with durations of 100-fs – 1-ps have been produced with the elimination second- and third-order dispersions by a number of laser systems. For ultrashort pulse systems (≤ 20-fs), however, the fourth-order-dispersion must be eliminated. This concern has been addressed by a number of groups, which have proposed and demonstrated dispersive optical systems that are capable of controlling dispersion up to fourth order [78-81]. For example, tests of the system described by Lemoff and Barty [79] indicate that broadening during the amplification and recompression of a 10-fs Gaussian pulse would be limited to less than 1-fs. With such a system, amplification of 10-fs optical pulses is therefore limited primarily by gain narrowing during amplification and the bandwidth of the optical components in the amplification chain.

The stretch factor in the expander-compressor combination system plays a key role in determining how close to the theoretical maximum quantum efficiency (TMQE), the amplification can be operated. In principle, if one considers the quantum defect and non-radiative losses, Ti:sapphire lasers which are pumped by frequency-doubled Nd:YAG lasers can achieve energy extraction efficiencies that approach ~ 57% of the pump pulse energy. Most Ti:sapphire CPA systems, however, achieve only 10 - 30% efficiency. To safely achieve TMQE, an amplifier must operate above the saturation fluence of the laser material [82] but below the intensity dependent damage threshold of the optical components in the amplification chain. For instance, to achieve efficiencies near the theoretical limit of Ti:sapphire, the fluence needs to reach ~ 2-J/cm^2 (twice the saturation fluence of Ti:sapphire). Saturating the gain in the amplifiers also stabilizes the pulse-to-pulse amplitude fluctuations. When operating at these fluences, the intensity in the amplifier must remain low to avoid intensity dependent breakdown of dielectric materials. This breakdown typically occurs at around an ~ 5-GW/cm^2 for optical coatings and stretched pulses in the ns-range. Dividing saturation fluence by maximum intensity without damage, we find that the pulse duration in the amplifier must be at least 200-ps and 1-ns for Ti:sapphire and Nd:glass, respectively in order to safely reach one times saturation fluence. Most Ti:sapphire CPA lasers use stretched pulse duration that are equal to or below 200-ps and are, therefore, unable to operate at the high fluences necessary for efficient amplification. In this paper we will present a Ti:sapphire system which stretches the pulses to order 1-ns and achieves final energy extraction efficiencies of >90% of TMQE.

Recent progress in ultrafast CPA systems has also utilized regenerative pulse shaping to counter gain narrowing [83, 84]. By including a frequency dependent filter to eliminate gain narrowing, regenerative pulse shaping allows the production of very short duration and high energy amplified pulses. With this technique the pulse duration of the amplified compressed pulses has been reduced by a factor of 2, reaching now 16-fs at a 10-TW level [44].

3. DESIGN, PERFORMANCE AND CHARACTERIZATION OF A 100-TW, SUB-20-FS, 10-HZ TI:SAPPHIRE LASER SYSTEM

As an example, the design, performance and characterization of a compact three-stage Ti:sapphire CPA laser system at the Advanced Photon Research Center (APRC), Japan Atomic Energy Research Institute is described in this section. The laser system is the front end of a 4-stage amplification system which is planned to eventually produce peak powers on the order of one petawatt (20-J in 20-fs). A schematic of the laser system is shown in Fig. 2. The system consists of a 10-fs Ti:sapphire oscillator, a cylindrical-mirror-based pulse expander, a regenerative amplifier incorporating regenerative pulse shaping, a 4-pass preamplifier, a 4-pass power amplifier and a vacuum pulse compressor.

3. 1 LASER SYSTEM FRONT END

Seed pulses were derived from an all-solid-state mirror-dispersion-controlled (MDC) Ti:sapphire oscillator which is capable of producing ~ 10-fs pulses [85]. The repetition frequency of the oscillator is 82.7-MHz. The pump laser is a 5-W frequency-doubled cw diode-pumped Nd:YVO_4 laser (Spectra-Physics, Millennia). Stable mode locking can be achieved with 4-W of pump power. The FWHM bandwidth of the pulses is ~ 120-nm. The interferometric autocorrelation of the pulses has been measured using a dispersion-balanced interferometric autocorrelator which is capable of measuring pulses down to 5-fs in duration. The FWHM pulse duration of the mode-locked pulses is typically 10-fs assuming a $sech^2$ envelope. In addition the phase and amplitude noise characteristics of the Ti:sapphire laser were greatly improved by using the diode-pumped solid state laser as a pump source [86].

Before amplification, the pulses from the oscillator were stretched by a factor of 100,000 in an all-reflective, cylindrical-mirror-based pulse expander [79]. The expander consists two gold-coated 1200-groove/mm ruled gratings, two cylindrical mirrors with a 1-m radius of curvature, a roof mirror and a horizontal image inverter. This design allows the compensation of dispersive phase errors up to fifth-order and eliminates

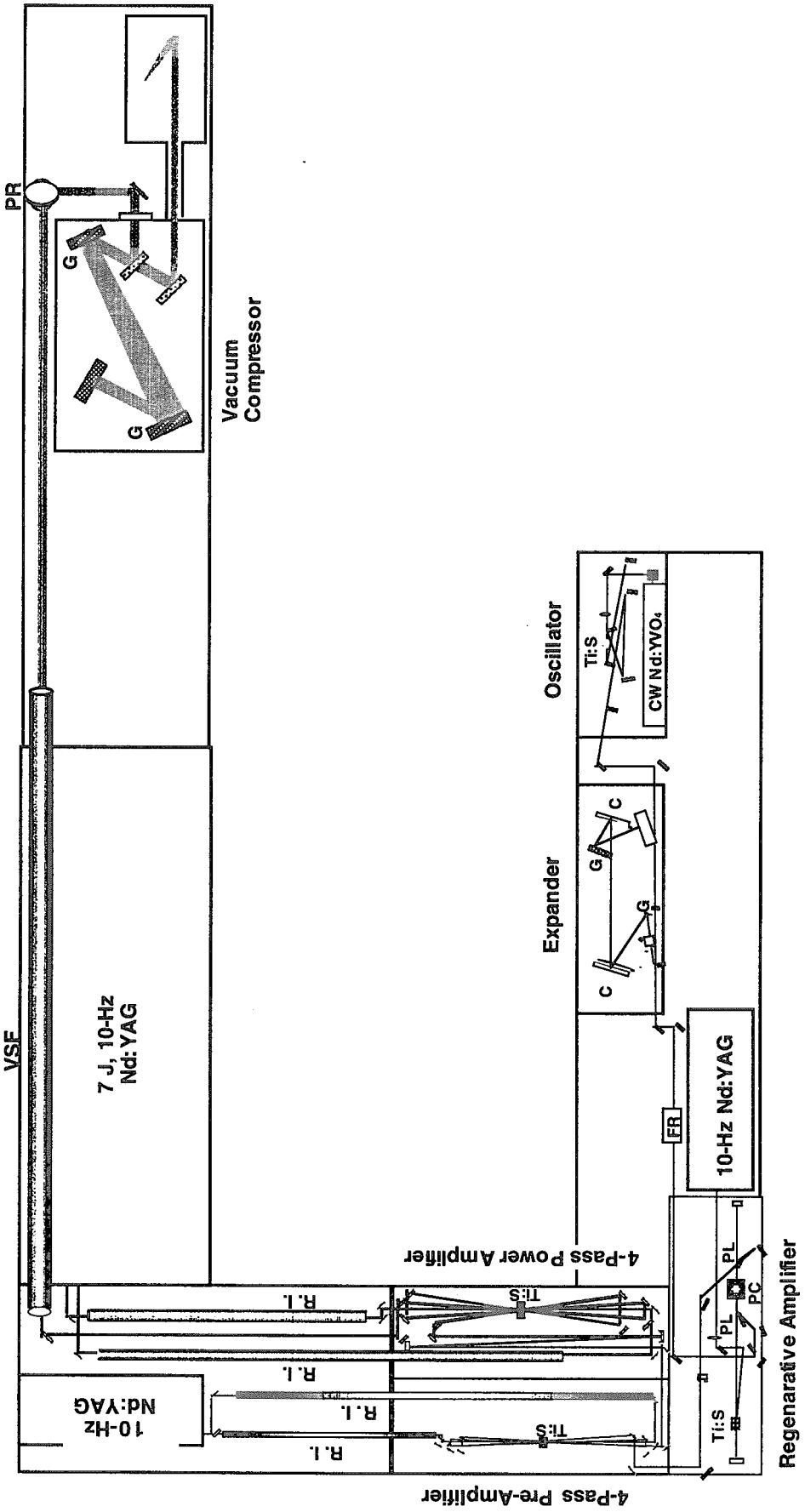

Fig. 2 An optical layout of a 100 TW, sub-20 fs Ti:sapphire laser system. Ti:S's, Ti:sapphire crystals; G's, gratings; C's, cylindrical mirrors; F. R., Faraday rotator; PC, Pockels cell; PL's, thin film polarizers; R. I., relay imaging optics; VSF, vacuum spatial filter; PR, periscope polarization rotator.

inhomogeneities. In order to calculate the dispersive characteristics of the expander, materials in the amplifier chain and the compressor, we use a dispersive ray-tracing analysis. By calculating the phase distortions of the bulk material such as Ti:sapphire, BK7 glass, KD*P, dielectric coatings and other dispersive elements in the laser system, we were able to determine the optimum settings of the grating separations and grating incidence angles for the expander and compressor that compensate the phase distortions and allow the pulse to recompress close to the transform limit. The bandpass of this expander is roughly 140-nm. The FWHM duration of the output of the expander is over 1-ns. Note that in this arrangement the pulse double passes the expander, i.e. is incident upon grating surfaces 8 times, before exiting. After passing through the expander and Faraday isolator, the stretched pulses are amplified in the regenerative amplifier.

We have installed a pointing-stabilizer system in the front end of the laser system. The system consists two piezo-driven reflection mirrors and two quadrant photodiode position-sensitive detectors which is similar to those in Ref. 87. The seed pulse from the oscillator is brought to the pulse expander using two piezo-driven mirrors providing of the resolution of 3 μradians, sufficient to control long term environmental drifts. By using this, beam wander of the seed pulse to the regenerative amplifier is reduced from 110-μradians root-mean-square (RMS) to 5.6-μradians RMS, thus greatly improving the long term stable operation of the laser system.

3. 2 REGENERATIVE PULSE SHAPING

If the saturation is negligible, the amplified spectrum of the pulse, *Iout(w)*, is determined by [88],

$$Iout(w) = Iin(w)\,[T(w)\,G(w)]^{N} \qquad (2)$$

where *Iin(w)* is the input spectrum of the pulse, *G(w)* is the frequency-dependent small signal gain, *N* is the number of passes, and *T(w)* is the frequency-dependent single-pass transmission function of the amplifier. In most terawatt CPA systems, a net gain of $>10^8$ is necessary to reach the desirable output pulse energy. Even though Ti:sapphire is the broadest bandwidth material as described in Section II, because of the frequency dependent gain profile *G(w,* amplification leads to gain narrowing of the pulse spectrum. A reduction in gain bandwidth not only reduces the stretched pulse duration but also results in a longer pulse after compression. The spectrum which results from seeding the amplifier with infinite bandwidth, zero energy pulses has been termed the "gain narrowing limit" of the system. Systems which include frequency dependent, lossy elements, such as polarizers

and Pockels cells, will require more total small signal gain to achieve the same output energy and will thus experience more gain narrowing. For this reason, regenerative amplifiers tend to limit amplified bandwidths more than multipass amplifiers. Therefore, conventional wisdom is that multipass amplifiers are better than the regenerative amplifier in terms of spectral narrowing.

Equation (1), however, suggests three ways to alleviate gain narrowing. First, the gain bandwidth of the amplification medium could be increased. A number of groups have attempted to increase the effective gain bandwidth of the amplification medium through mixed gain media with different peak gain wavelengths in Nd:glass [88, 89]. In this way pulses as short as 275-fs have been generated in a Ti:sapphire/Nd:phosphate and Nd:silicate glass hybrid laser [89]. Second, while narrower spectra will experience less percentage narrowing, for fixed input energy, a larger input bandwidth will always result in a larger output spectrum. This fact is exploited by reshaping the pulse spectrum before amplification by increasing $I_{in}(\omega)$. Multiterawatt pulses with duration of 30-fs have been produced [54] in this manner by placing a spatial mask in the focal plane of the expander.

A third possibility is to introduce a frequency dependent loss during amplification with greater attenuation at the peak of the gain profile than in the wings. The net amplification on each round trip is small, typically 2 - 3. Therefore, gain narrowing can be compensated on each round trip by inserting a linear filter that selectively attenuates the pulse spectrum after each transit of the amplifier. This method is practical for systems that employ multiple passes of single gain medium since the gain narrowing on any one pass is also relatively small. This is conveniently accomplished in regenerative amplification schemes by placing a frequency dependent attenuator inside the regenerative amplifier cavity. We have tested birefringent filters, spatially masking in the dispersive end of a cavity incorporating a prism pair, angle-tuned thin etalons, angle-tuned air-spaced etalons, and thin film polarilzer etalon as spectral filters. In the sample amplification system, angle-tuned thin etalons are used in the regenerative amplifier to broaden the amplified spectrum beyond the gain narrowing limit.

A layout of the ultrabroadband regenerative amplifier is shown in Fig. 3. The regenerative amplifier is a stable TEM_{00} cavity and the resonator is 1.8-m long and uses two cavitymirrors. The cavity consists of a 10-m radius of curvature concave dielectric mirror, and a 20-m radius of curvature convex dielectric mirror. The MgF_2 anti-reflection (AR) coated Ti:sapphire crystal (Union Carbide Corporation) is 7-mm long with 0.15 wt.% doping. The crystal is end pumped with a frequency-doubled Q-switched Nd:YAG laser (Continuum, Powerlite 8010) that produces 7-ns pulses at a 10-Hz repetition rate. A 50-cm focal-length lens focuses the pump beam onto the Ti:sapphire crystal. Pulse injection in the regenerative amplifier is achieved by an intracavity Pockels cell (Cleveland Crystal Inc.)

placed between thin film dielectric polarizers (CVI Laser Corp.). The thin film dielectric polarizers have a single-pass transmission (Tp > 98%) from 700- to 950-nm. The Pockels cell is coated with a sol-gel material. A high voltage pulse generator (Medox E-O, Inc.) capable of producing up to ~ 6-kV pulses with a FWHM of 8-ns is used to drive the Pockels cell. A pulse is injected after reflecting off of one of the polarizers and passing through the Pockels cell which is pulsed with a half wave voltage coincident with the optical pulse arrival. After 12 round trips, the pulse is ejected from the cavity, having fully depleted the gain, by once again pulsing the Pockels cell to have a half wave voltage and reflecting off of the other polarizer. The amplified pulse energy is typically ~ 13-mJ.

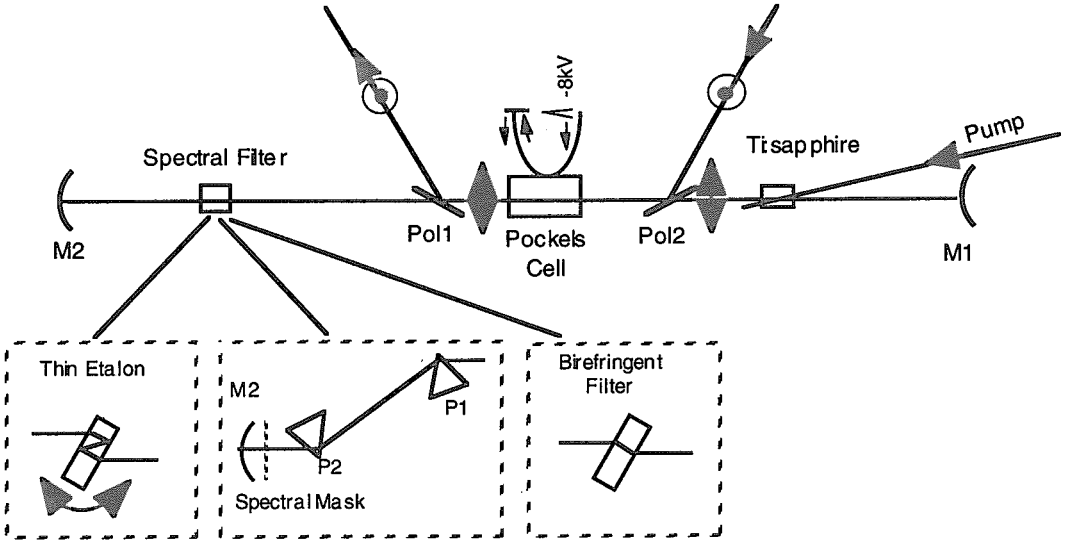

Fig. 3 Schematic of the regenerative amplifier with the spectral filters. Pol 1, 2, thin film polarizers; M1, -20 m dielectric mirror; M2, +10 m dielectric mirror.

Two, 3-μm thick etalons (Melles Griot Corp.) are used in transmission and are angle tuned so as to be off resonance (highest attenuation) around the peak of the gain profile centered at 790-nm. It should be noted that for a given thickness etalon which has been tuned to anti-resonance, there corresponds one value of single pass gain which gives a maximally flat spectrum. Higher values of gain produce narrower spectra and lower values produce double peaked spectra. The single pass gain is conveniently adjusted by changing the pump energy to the regenerative amplifier. The total output can be held constant by adjusting the number of cavity round trips. The amplifier output energy was adjusted to be approximately 8-mJ. When the stretched pulse was amplified in the regenerative amplifier without a spectral filter, the spectrum narrowed to 28-nm as shown

in Fig. 4. However, by using the etalons to produce a frequency dependent attenuation and selectively amplifying the wings of the spectrum, in the spectrum of the amplified pulse was broadened to 82-nm FWHM (Fig. 4). These etalons can however produce significant cubic phase error [44]. The delay is largely quadratic over most of the bandwidth of the pulse indicating that the predominant phase distortion is cubic. This predominantly cubic phase of the etalons as well as the cubic phase distortion of the high damage threshold mirror coatings (CVI Laser Corp.) has been compensated by slight alteration of the grating angle of incidence in the compressor.

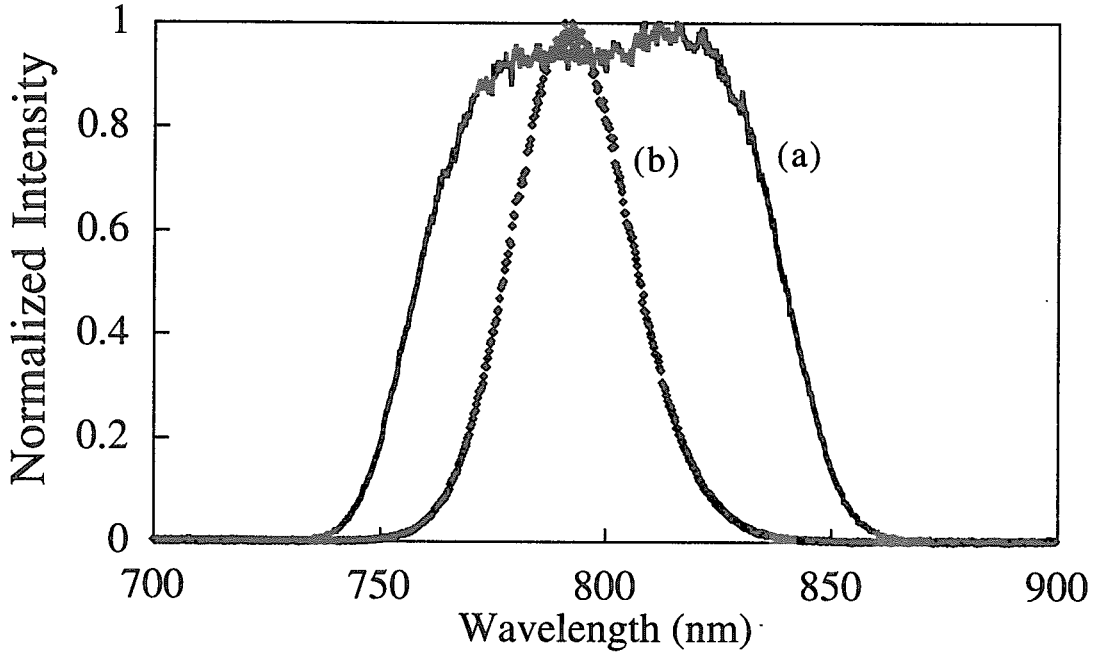

Fig. 4 The spectra for amplified pulses from the regenerative amplifier (a) with and (b) without the thin solid etalons.

In addition, it should be noted that modified filters also permitted the simultaneous amplification of two colors. Pulses centered at 765-nm and 855-nm have been amplified simultaneously without unwanted amplification at the peak of the gain profile as shown in Fig. 5. Such pulses should lead to compact sources of high power, tunable mid-infrared light via difference frequency mixing. It should also be possible to produce energetic, multi-wavelength, femtosecond pulses with this technique.

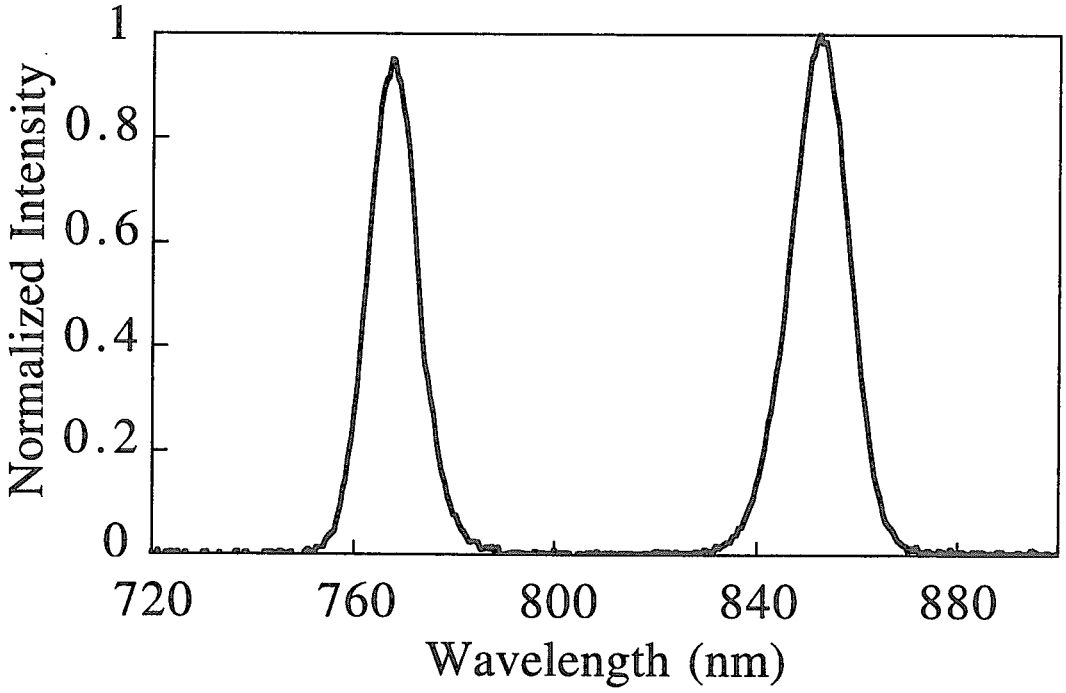

Fig. 5 Spectrum of two color pulses centered at 765 nm and 855 nm amplified simultaneously.

3. 3 MULTIPASS AMPLIFIERS PERFORMANCE

The 8-mJ output beam from the regenerative amplifier is enlarged by a Galilean telescope to an approximately 6-mm diameter. Further amplification is accomplished in a four-pass preamplifier. This amplifier uses a 20-mm diameter, 15-mm long, Ti:sapphire crystal (0.15% doping, Union Carbide Corporation) with MgF_2 AR coatings on both faces. The amplifier is pumped with 532-nm pulses from a frequency-doubled, Q-switched Nd:YAG laser (Continuum, Powerlite 9010) that produces, 690-mJ, 7-ns pulses at a 10-Hz repetition rate. The beam from the pump laser is split into two outputs, which are then relay imaged to opposite faces of the amplifier crystal. Relay imaging optics with a demagnification (M = 0.67) provide spatially uniform pump beams with diameters of ~ 6-mm at both faces of the crystal. The signal and pump beams propagate in a near collinear manner to maximize the gain and absorption, respectively. Since thermal lensing occurs in the Ti:sapphire crystal at ~ 7 W average pump power, the beam diameter on the last pass is decreased to ~ 4.5-mm. For high efficiency, the pulse fluence on the last pass in the amplifier was designed to be ~ 1.6-J/cm^2. The resulted output pulse energy was ~

320-mJ. This amplifier provides total saturated gain of 40. The small signal gain in the amplifier has also been measured to be 3.7.

The output of the preamplifier is up collimated to an ~ 18-mm diameter with a Galilean telescope and then introduced into the four-pass power amplifier. This amplifier uses a water cooled 40-mm diameter 25-mm long Ti:sapphire crystal (Union Carbide Corporation) with anti-reflection coatings on both faces and is pumped with a custom built Nd:YAG laser which is capable of producing ~ 7 J of 532-nm radiation at 10-Hz.

Output of conventional Ti:sapphire CPA systems, is typically limited in energy and average power to few hundred millijoules and several watts. This is primly due to the limited energy and average output power of commercially-available, flash-lamp-pumped Nd:YAG lasers which produce maximum outputs of order ~ 1-J and ten watts. Nevertheless, a ultrashort pulse Ti:sapphire laser which generates pulses of ~ 25-TW peak power and ~ 30-fs duration at a 10-Hz repetition rate pumped by three Nd:YAG lasers [39] has been demonstrated. In addition, a high energy amplifier system based on single-shot Nd:glass pumped Ti:sapphire has also delivered ~ 1.1-J pulses with 120-fs duration [57]. Because the first laser system requires large number of pump lasers, however, cost and complexity are high. The second system is limited in repetition rate, because the Nd:glass pump laser can only be fired every 4 minutes. To obtain greater than 3-J of energy from the Ti:sapphire disk at 10-Hz requires a pump laser with > 6-J of energy and > 60-W of average power at 532-nm. For this purpose we have developed a flash-lamp-pumped high energy and high average power Nd:YAG laser.

The pump laser uses Nd:YAG rod amplifiers up to a diameter of 12-mm in the master oscillator - power amplifier (MOPA) configuration. The goal of this type of pump laser design is to extract as much energy as possible and to ensure the high frequency conversion efficiency while maintaining a uniform spatial beam profile. This had been previously accomplished with relay-imaged amplifier chains in large scale Nd:glass laser systems [90]. In this architecture a master oscillator generates tens of nanosecond pulse of several hundred millijoules that is then spatially shaped and split into parallel chains of single-pass rod amplifiers of increasing size. Faraday isolators and Pockels cells are used to isolate pulses from propagating backward down the laser chain. The amplifier chains are separated by relay telescopes or spatial filters that reimage a beam forming aperture at several places through the amplifier chains. Our custom pump laser uses a similar architecture and consists of an oscillator, a preamplifier chain, two power amplifier chains and two frequency doubling crystals. 18-ns pulses from a long cavity single-longitudinal-mode Nd:YAG oscillator, are passed through a Faraday isolator and the soft aperture. The pulses are then relayed with a spatial filter (M = 1.0) through Nd:YAG amplifier rods of 9-mm diameter. A relatively long duration pulse compared with most Q-switched

Nd:YAG lasers enables the Ti:sapphire amplifiers to be pumped at high fluence level without intensity-dependent, 532-nm damage to the Ti:sapphire crystal. Next, the 470-mJ output pulses pass through two Pockels cells and are split into two beams. Each beam is further amplified in four 12-mm-diameter Nd:YAG rod amplifiers. Energies up to 7-J per beam in the IR have been achieved. Four relay imaging optics per arm (M = 2.0 and M = 1.0) are used to relay the images into those 12-mm rod amplifiers and the frequency doubling crystals. Faraday isolators and Pockels cells are used to prevent parasitic oscillation (PO) and amplified spontaneous emission (ASE) between the amplifiers. Ninety degree rotators placed between first and second 12-mm rod amplifiers, third and fourth 12-mm rod amplifiers are also used to cancel the birefringent depolarization introduced by the amplifiers. The IR outputs from the power amplifier chains are frequency doubled to 532-nm using type II KD*P crystals. The conversion efficiency defined as the green energy output from the crystal divided by the IR energy input to the crystal was ~ 50% which yields output pulse energy of ~ 3.5-J per pulse at 532-nm. Figures 6 (a) and (b) show vertical and horizontal cross sections of a typical pump beam profile image on the Ti:sapphire amplifier crystal, respectively.

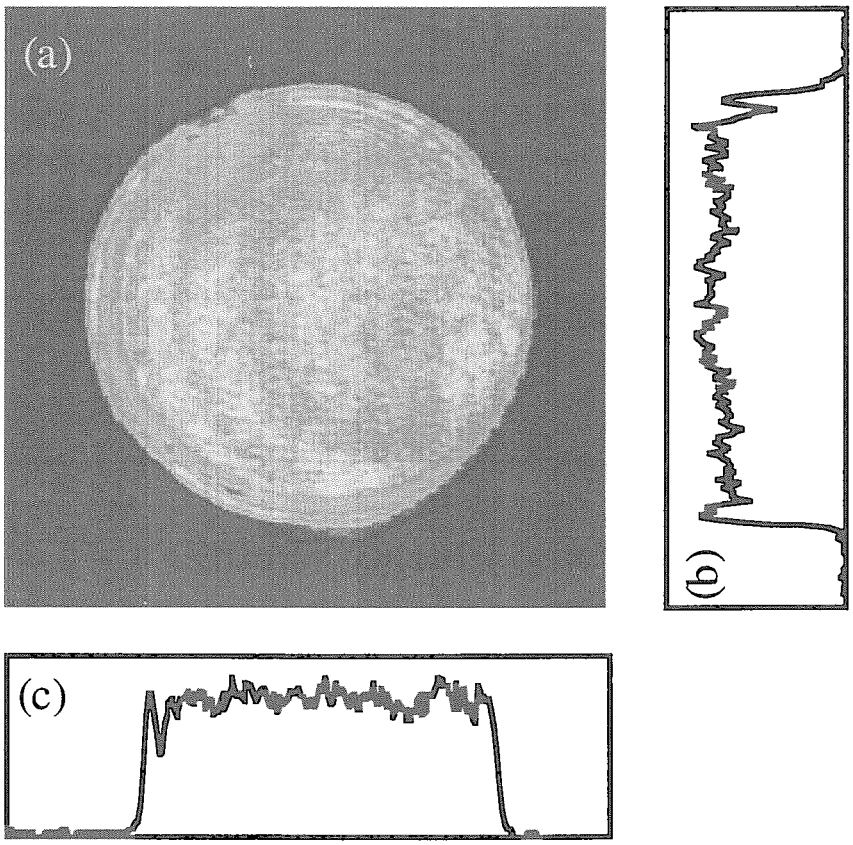

Fig. 6 (a) Nd:YAG pump beam profile imaged on the Ti:sapphire power amplifier crystal. (b) Vertical and (c) horizontal cross sections of the profile, respectively.

The saturation characteristics for the frequency-doubled Nd:YAG laser pumped power amplifier are shown in Fig. 7. The three curves are the calculated efficiencies of the power amplifier as a function of pump pulse fluence at different input pulse fluences based on a Frantz-Nodvic simulation [82]. Squares, circles and a triangle represent the measured efficiencies in the power amplifier. With 6.4-J of pump light incident upon the crystal the amplifier has produced 3.3-J of 800-nm radiation. This amplifier provided a total saturated gain of 10 and a small signal gain of ~ 5. Under these conditions, this amplifier has reached 90% of the theoretical maximum conversion efficiency of 532-nm pump light to 800-nm radiation. Nearly identical extraction efficiencies have also been recently obtained from a similar laser at the University of California, San Diego [59]. These results agree well with our model calculation [91].

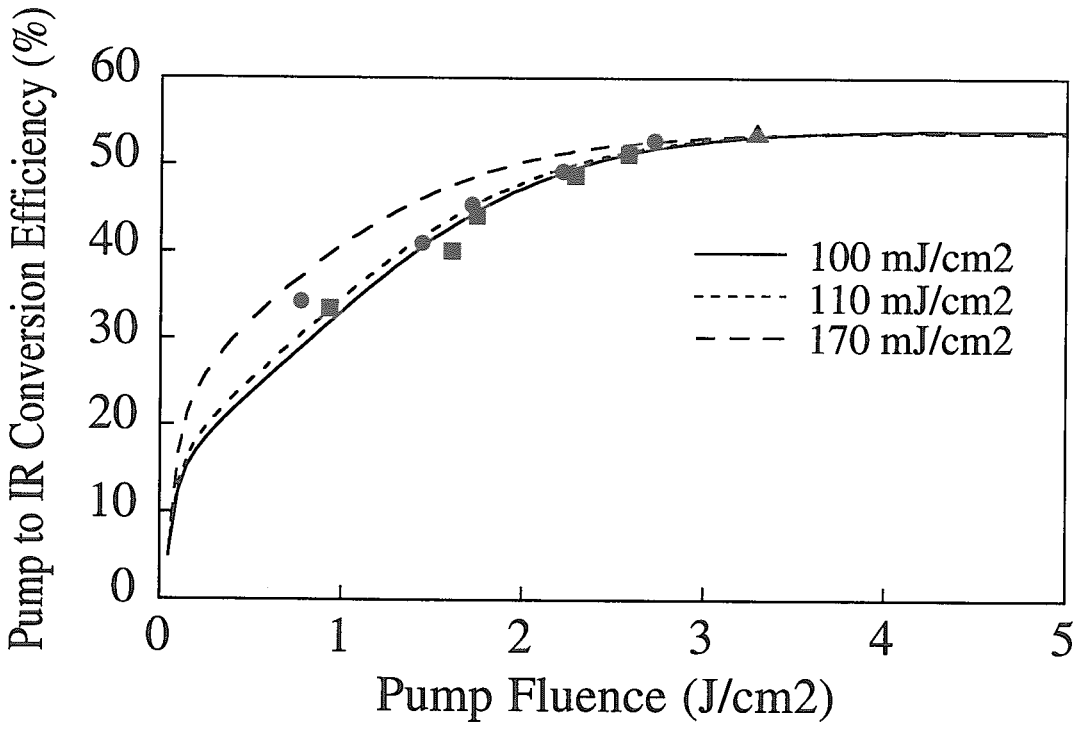

Fig. 7 Saturation characteristics for the Ti:sapphire power-amplifier. The three curves are the calculated efficiencies of the power amplifier as a function of pump pulse fluence at different input pulse. Squares (input fluence of 96 mJ/cm^2), circles (input fluence of 115 mJ/cm^2), and a triangle (input fluence of 168 mJ/cm^2) represent the measured efficiencies in the amplifier.

One important note in operating a Ti:sapphire amplifier with such high fluences is that the amplified pulse spectrum is reshaped and red-shifted due to saturation. In this case, it is not desirable to center the wavelength of the pulses at 800-nm in the regenerative and pre- amplifier stages, since the effect of gain saturation causes the pulse spectrum to show an appreciable red-shift with respect to the peak of the gain spectrum of the power amplifier. Instead, a broad amplified bandwidth at high-energy output was obtained by shifting the spectrum of the input toward the short wavelength side of the desired output. This was accomplished by slight tuning the incidence angle of one of the etalons in the regenerative amplifier (Fig. 8).

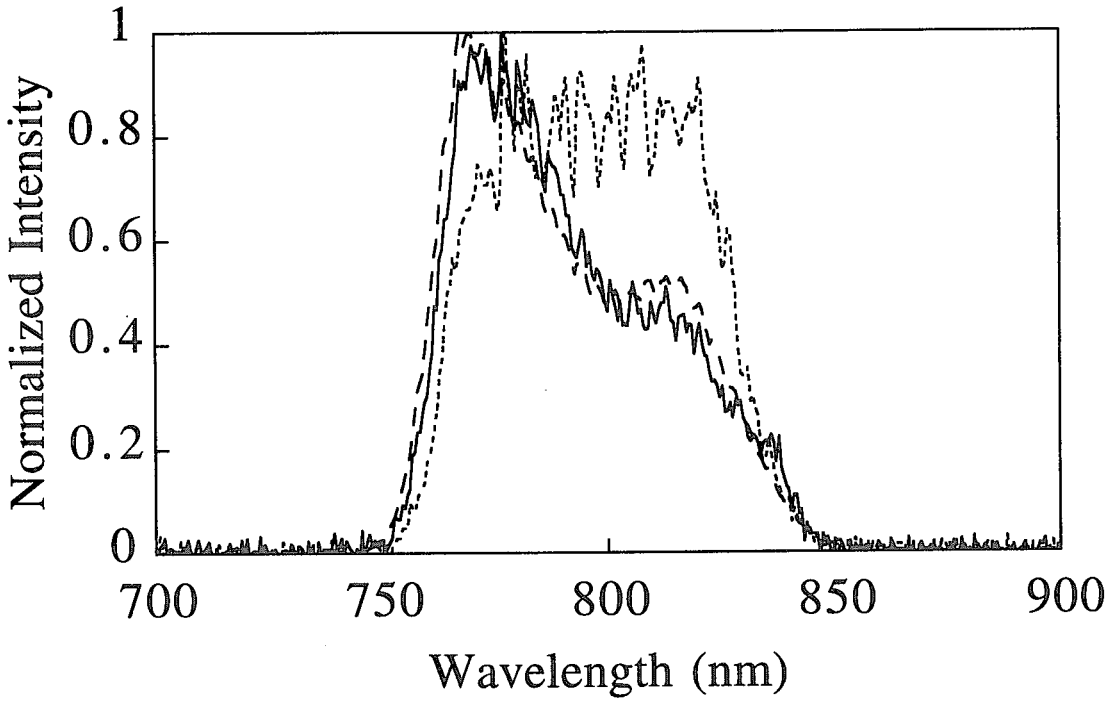

Fig. 8 Measured amplified spectrum after the regenerative amplifier (solid line), the 4-pass pre-amplifier (dashed line) and the 4-pass power-amplifier (dotted line), respectively.

We have checked the thermal lensing effect in the power amplifier under full power operation. To obtain near-field and far-field beam profiles lenses with a focal length of f = 1-m were placed just after the amplifier and at 7.6-m away from the amplifier, respectively. These profiles were recorded on the CCD cameras. The thermal lens in the horizontal plane is about f = + 25-m whereas it is f = + 9.5-m in the vertical plane. This difference between two planes may be caused by inhomogeneties of the Ti:sapphire crystal or thermal

aberration in the crystal. To compensate for this lensing in the vertical plane, we placed a cylindrical mirror of f = - 9-m just after the preamplifier.

3．4 PULSE COMPRESSION AND TEMPORAL CHARACTERISTIC

The output of the power amplifier passes through relay imaging optics with a magnification (M = 3.3). This provides a spatially uniform beam for the pulse compression gratings and collimates the beam diameter to an approximately 50-mm. The vacuum pulse compressor consists of two parallel, gold-coated, 1200-grooves/mm, ruled gratings (Richardson Grating Labs.), which had a measured diffraction efficiency of ~ 91%.

A fraction of the compressor output was sent to a single-shot autocorrelator, which utilized a 50-μm BBO doubling crystal. The FWHM of the measured pulse duration is 18.7-fs. The duration of the transform limit, as calculated from the measured, amplified spectrum after the compressor is 17-fs. The high degree of agreement suggests that the compressed pulses are nearly transform limited. The transmission of the compressor, including the multilayer dielectric- and gold-coated turning optics, was ~ 57%, yielding a compressed output pulse energy of 1.9-J, which implies a peak power for the laser pulse in excess of 100-TW. Because gain saturation in the amplifier stabilizes the pulse-to-pulse amplitude fluctuation, the energy stability is typically less than ±2%. The final output energy that is achievable from the laser system is limited by the damage threshold of the pulse compression gratings. The first grating has been operated at a fluence of 80-mJ/cm^2, an average power density of 0.8-W/cm^2 and a peak power density of 2.5-TW/cm^2, respectively, with no indication of damage on the grating.

In high-field physics experiments, such a pedestal and/or ASE would create a low density plasma in advance of the main laser pulse and thus significantly alter the physics of the laser/matter interaction [92-94]. Therefore detailed characterization and control of the temporal shape and phase of the laser pulse is crucial to the study of high-intensity laser-matter experiments. For this purpose, the phase and contrast of the laser pulse were measured with the techniques of second harmonic generation (SHG) Frequency Resolved Optical Gating (FROG) [95-98] and high dynamic range cross-correlation [99].

The nonlinear material used in the SHG FROG was a 100-μm thick KDP crystal. The SHG signal was detected by an imaging spectrometer (Acton Research Corporation: SP-150-S) with a grating of 300 groove/mm and a CCD camera (Princeton Instruments: TE/CCD-512-TKM/1PI - 512 × 512 pixels). The sensitivity as a function of the wavelength of the detection system was calibrated by using a Halogen lamp (Ushio: JPD-100-500CS). The measured FROG trace was extracted using the central 256×256 pixel

area of the CCD camera and then retrieved until the FROG error decreased to less than ~ 0.01. The number of iterations was 20 in this case. Figure 9 (a) shows the pulse intensity and phase in time retrieved from the SHG FROG trace. The pulse duration is 20-fs full width at half maximum (FWHM) accompanied with pre- and post-pulses. The intensity and phase of the pulse in frequency are also shown in Figure 9 (b). The spectral width is 67-nm FWHM. Each term of phase distortion was determined by polynomial fitting to the spectral phase of the FROG measurement. The measured pulse contains of a group delay dispersion (GDD) of 2.83×10^{2} fs^{2}, a cubic phase of 3.73×10^{3} fs^{3}, and a quartic phase of 3.80×10^{6} fs^{4}. Based on these results, we conclude that the predominant phase distortion is quartic.

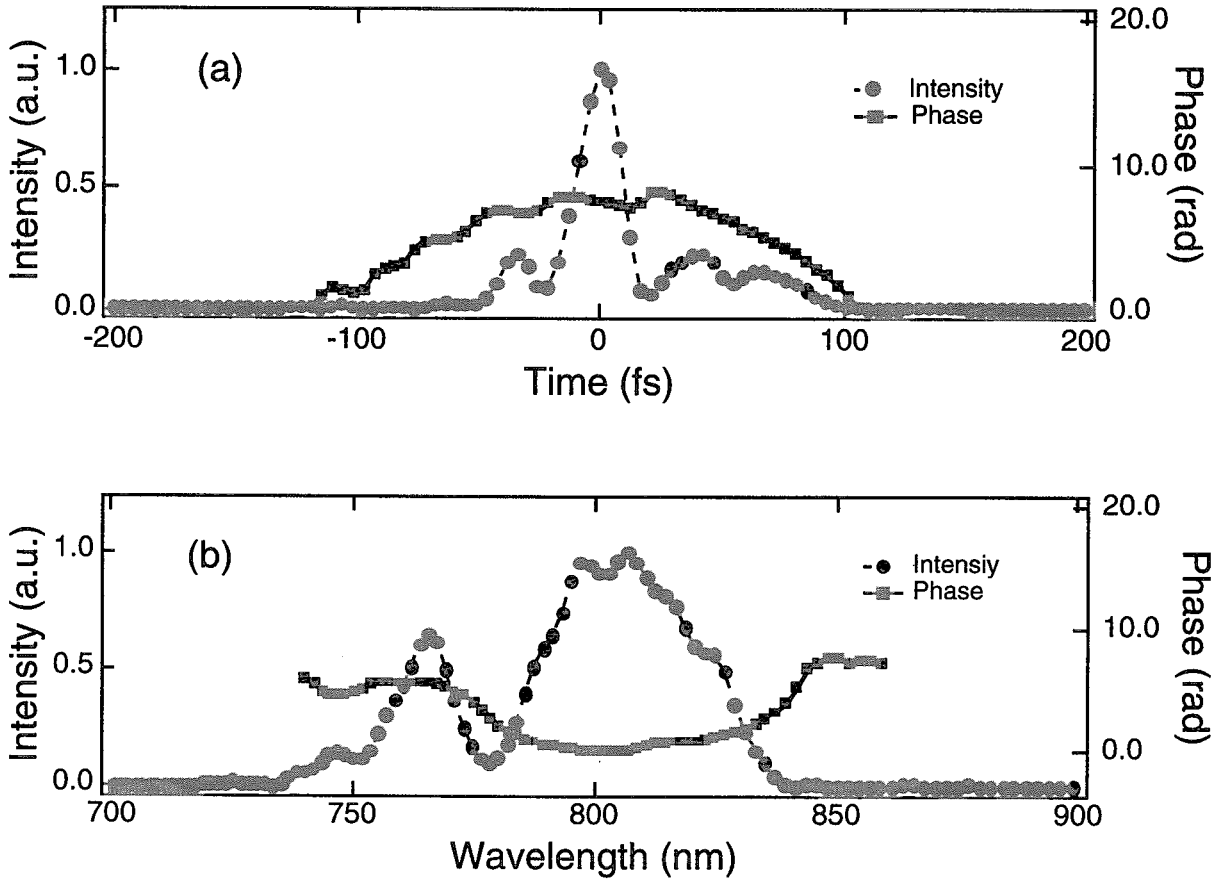

Fig. 9 Retrieved intensities and phases of the SHG FROG trace for the compressed pulse. (a) Pulse intensity (circles) and phase (squares) in time. (b) Spectral intensity (circles) and phase (squares) as a function of wavelength.

Minimization of the total phase error can be achieved by balancing the phase terms of the GDD and quartic [100, 101]. In Ref. 101, an optimization algorithm is used to find the best setting for as many variables as experimentally available. We then apply to the experimental result of SHG FROG measurement for the total phase simulation. The modified total phase of $\phi_{(\omega)}^{Mod}$ is determined from the experimental result of $\phi_{(\omega)}^{FROG}$ by

$$\phi_{(\omega)}^{Mod} = \left(\phi_{(\omega)}^{FROG} - \phi_{(\omega)}^{Comp}\right) + \phi_{(\omega)}^{CompN}, \qquad (3)$$

where $\phi_{(\omega)}^{CompN}$ is the phase term introduced by the new compressor. In Eq. (3), the phase term $\phi_{(\omega)}^{FROG}$ - $\phi_{(\omega)}^{Comp}$ represents the phase including the expander and amplifier components in the laser system. We then calculate the modified total phase as a function of $\omega - \omega_0$ for various settings of the separations and incidence angles for the new compressor gratings. The values of the root mean square (RMS) and the peak to valley of the modified total phase as a function of $\omega - \omega_0$ are also calculated for each setting.

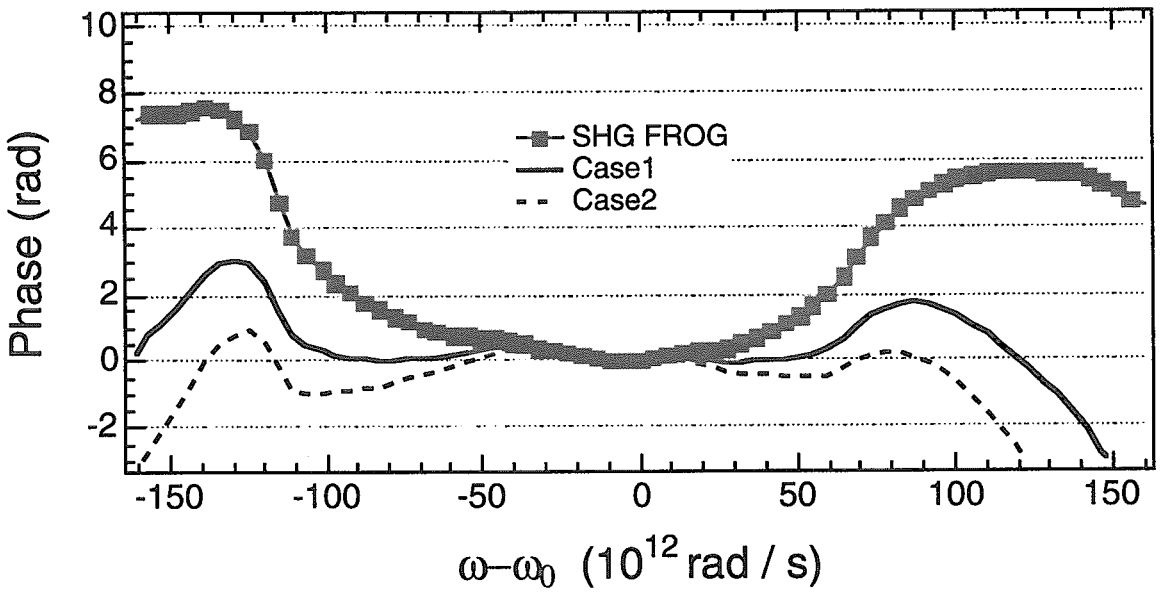

Fig. 10 Measured (SHG-FROG) and calculated (Case 1 and Case 2) total phases as a function of $\omega - \omega_0$. Case1 and Case 2 minimize the RMS and peak to valley of the modified total phases as a function of $\omega - \omega_0$, respectively.

Figure 10 shows the experimental result of spectral phase (circle) which is the measured value as shown in Fig. 9 (b) and modified total phases (solid and dashed lines). Two cases are found in order to make the modified total phase as flat as possible. The separations and incidence angles of the compressor gratings of two cases correspond to 115.192 cm, 62.95° (Case1: solid line) and 115.179 cm, 62.94° (Case2: dashed line), respectively. In Case1 the RMS of the modified total phase as a function of ω-ω_0 is minimized. In Case2 the peak to valley of the modified total phase as a function of ω-ω_0 is minimized. In this simulation, Case1 is better in terms of the reduction of pre- and post-pulses than Case2, although the pulse durations of these three cases are almost unchanged. The level of the prepulse occurring ~ 35 fs before the main pulse using the parameters of Case1 can be reduced below to half that of the experimental value. More precise control of the total phase can also be realized by using an active phase compensator. For example, a deformable mirror can be used for an ultrashort pulse laser system as an active phase compensator [102].

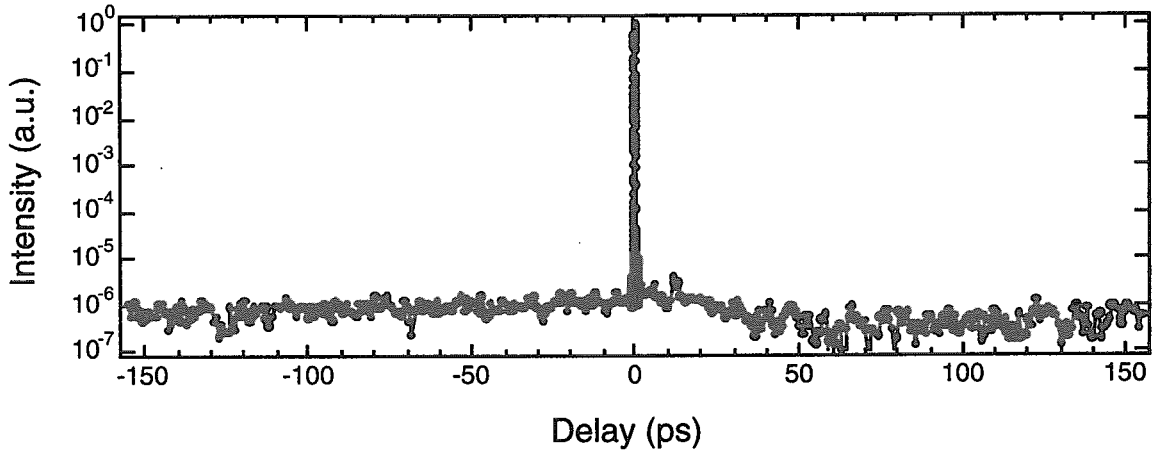

Fig. 11 High dynamic range cross-correlation trace of a compressed pulse. Each point of the cross-correlation trace corresponds to an average of ten laser shots.

The arrangement of the cross-correlator is that of a Type I phase-matched, noncollinear geometry which incorporates SHG and THG nonlinear crystals. The SHG and THG signals were obtained with 1-mm and 500-μm thick KDP crystals, respectively. The THG signal was then recorded by a standard photomultiplier tube (PMT, Hamamatsu: H6780-06). A computer controlled stepping-motor (Newport: M-UTM50PP) was used to vary the delay between the two cavity arms (up to ±160-ps). Calibrated neutral density filters were also used to obtain the THG signals at a different attenuation level. The signal from the PMT was time gated (50-ns) to avoid any other long-time-scale noise and averaged

over ten laser shots in a Boxcar integrator (Stanford Research Systems: SR250). The cross-correlation signal of the compressed pulses is shown in Figure 11. Each point of cross-correlation trace with a time resolution of 670-fs corresponds to an average of ten laser shots. The detection limit of this apparatus is approximately 10^{-8}. The measured contrast is of the order of 10^{-6} limited by ASE mainly coming from the regenerative amplifiers. ASE can be easily suppressed by two orders of magnitude by using a solid-state saturable absorber with a preamplifier before the pulse expander [102].

3．5 SPATIAL BEAM QUALITY AND WAVE-FRONT CHARACTERISTIC

Since the CPA laser systems are now approaching focused laser intensities of 10^{20} - 10^{21} W/cm^2, the quality of the beam corresponding to diffraction limited spot size is crucial. The spatial beam quality was determined by focusing the attenuated output with a 3-m focal-length spherical mirror and measuring the spot size at the focus with a CCD camera. Under the full power operations of the laser system, the spatial quality of the beam produced a spot which was 2- and 2.5-times that of a diffraction limited gaussian beam in vertical- and horizontal-planes, respectively. We have determined that approximately 80% of the focused energy lies within the spot. With an f/3 off-axis parabolic mirror, focused intensities of ~ 3 x 10^{20} W/cm^2 should be possible with this beam quality.

While a focused beam profile can be taken with a CCD camera as mentioned above, a measurement of the spatial phase of the laser beam is more useful from a viewpoint of improving the beam quality. Such measurements can be used to provide input to active phase correction schemes using deformable mirrors. Several phase measurement methods such as Shack-Hartmann wave-front sensors and lateral shearing interferometers have already been proposed and demonstrated [104-107]. We have recently demonstrated that single-shot wave-front measurements of high-peak-power femtosecond laser pulses by using the Fresnel phase retrieval method [108]. The wave-fronts are reconstructed from only two intensity distributions at two planes along the optical axis, which are measured by means of simple CCD cameras.

The Fresnel phase retrieval algorithm is based on the Gerchberg-Saxton [109] and the Fienup [110-113] phase-retrieval algorithm. Assuming that the monochromatic laser beam propagates along the z-axis and the two amplitudes measured at the two positions of z=0 and $z = Z$ are $u_0(x,y)$ and $u_Z(x,y)$, respectively, where Z is the distance between the two measured points, this algorithm would consist of the following five steps: (1) the amplitude measured at z=0 and an initial phase given by uniform distribution, (2) propagate through the distance + Z, (3) replace the amplitude with the amplitude measured at $z = Z$, leaving the phase unchanged, (4) propagate through the distance - Z (i.e., inverse propagation

through the distance + Z), (5) replace the amplitude with the amplitude measured at z = 0, leaving the phase unchanged. This iteration loop (2) - (5) is repeated until the root-mean-square (RMS) error of intensity distribution decreases to an acceptable level, and then the phase distribution at z = 0 (or z = Z) is retrieved. In this algorithm, the propagation calculation in the Fresnel region is implemented by a convolution integral with a convolution kernel depending on the propagating distance Z [114]. For the inverse propagation, the distance Z is substituted with - Z.

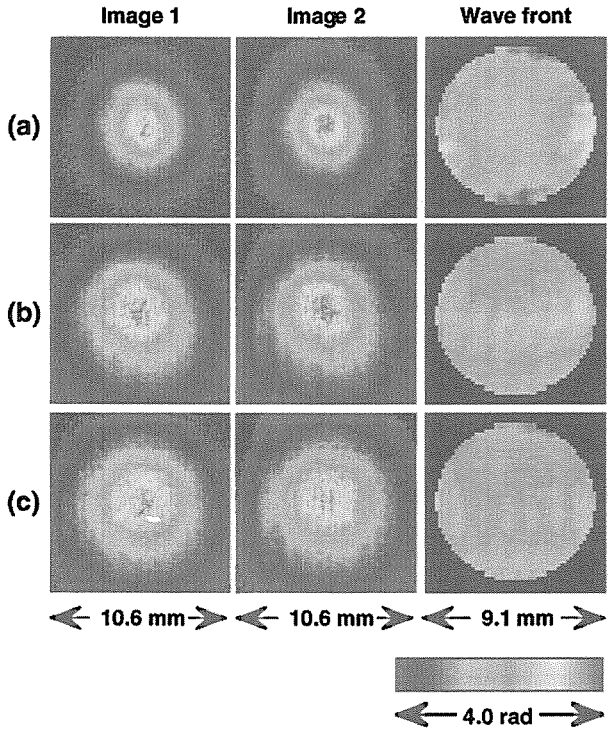

Fig. 12 Two measured two intensity distributions (Image 1 and Image 2) and the reconstructed wave-fronts of the 100 fs pulses at different output power levels. The output energies of the four-pass amplifier were (a) 42 mJ and (b) 2 mJ both with 450 mJ pump lights and (c) 2 mJ with 210 mJ pump light, respectively. The reconstructed wave-fronts were measured to be (a) 0.36 λ PV and 0.05 λ RMS, (b) 0.22λ PV and 0.03λ RMS, and (c) 0.25λ PV and 0.04λ RMS, respectively.

Figure 12 shows the two measured intensity distributions and the reconstructed wave-fronts of the 100-fs pulses at different output power levels. Output energies of the Ti:sapphire amplifier were controlled by changing the timing of the flash-lamps of the pump laser in the case of Fig 12 (a) and 12 (b) and by changing the pump energy in Fig. 12 (c).

Output energies were 42-mJ in Fig. 12 (a) and 2-mJ in Fig. 12 (b) both with 450-mJ pump energy and 2-mJ in Fig. 12 (c) with 210-mJ pump energy, respectively. The wave-fronts are somewhat deformed with increasing the output energy of the amplifier mainly due to thermal aberrations in the Ti:sapphire amplifier crystal. Because of these distortions, the beam diameter for 42-mJ output [see Fig. 12 (a)] was reduced to ~ 6.5-mm compared to the initial 8-mm diameter beam. The accumulated B-integral through the laser system was also estimated to be 0.07 in Fig. 12 (a) and less than 0.01 in Fig. 12 (b) and 12 (c), respectively. The reconstructed wave-front of the 42-mJ output, corresponding to terawatt-level output peak power after compression, was 0.36λ PV and 0.05λ RMS, respectively. The spot diameter of the measured focused beam of this high peak power pulse was measured to be ~ 170-μm, corresponding to a 1.04 and d 1.07 times diffraction limited in vertical- and horizontal-planes, respectively and agreed with the calculated FFP.

We are currently implementing this method on the 100-TW Ti:sapphire laser chain. We also believe that the wave-front correction of laser beams could be achieved with a deformable mirror with the diagnostic technique described in this section.

4. TOWARDS A PETAWATT

The potential scalability of ultrafast CPA architectures described in this paper to higher energies is an important issue considering peak powers up to the petawatt level. To scale the system to peak powers above 100-TW requires larger size gain media, higher energy pump lasers and larger diameter gratings. In this section, we discuss these issues including of suppression of parasitic oscillation across the large-aperture Ti:sapphire amplifier disk, optimization of the spectrum of the amplified pulse at the output of the amplifier and compensation of high-order dispersion in the laser chain.

4. 1 SUPRESSION OF TRANSVERSE, PARASITIC OSCILLATION

Ti:sapphire disks with up to 100-mm in diameter are available with current growth technologies [115]. To obtain greater than 40-J of energy from this Ti:sapphire disk requires a pump laser with ~ 70-J of energy. We present here the calculated results of the Ti:sapphire booster amplifier, which is based on Frants-Nodvic simulation [82]. The goal of performing these calculations is to achieve higher amplifier efficiencies under parasitic oscillation threshold, and to determine an optimum beam diameter in the amplifier crystal and the number of passes in the multipass configuration. The booster amplifier will use an 80-mm-diameter 33-mm-long Ti:sapphire crystal (Crystal Systems Inc.) with antireflection coatings centered at 800-nm on both faces and the Ti:sapphire crystal will be pumped on

both sides with a custom-built single-shot Nd:glass laser that is capable of producing ~ 75-J energy at a 532-nm radiation. The 532-nm absorption coefficient of the crystal is ~ 0.85/cm. In this calculation, we assume the entire pump energy is fixed at 70-J and the beam diameter of 532-nm pump light is equal to that of 800-nm incident light. Thus, the pump fluence would depend only on the diameter of the pump light.

The major problem with a high-energy laser amplifier such as the this final booster amplifier is parasitic oscillation and ASE across the large-aperture amplifier disk at high-energy pump fluences. Parasitic oscillation is due to the Fresnel reflection at the transverse material interfaces of the gain medium. Above the parasitic oscillation threshold, transverse spontaneous emission lases and the gain is clamped, no additional energy can be stored in the amplifier, and the amplifier efficiency is thus significantly reduced. These phenomena have well been studied and characterized in large-aperture Nd:glass disk amplifiers [116, 117]. For Nd:glass, techniques for parasitic mode suppression include using absorbative glass claddings to lower the disk edge reflectivity. This technique has successfully suppressed parasitic oscillations even in very large aperture (> 30-cm in diameter) Nd:glass amplifier disks. Unfortunately, suppression of parasitic oscillation in Ti:sapphire is more difficult due to the significantly higher refractive index (n = 1.76) which leads to higher Fresnel reflection at the interfaces and due to the relatively large transverse gain present in final amplification stages. Nevertheless, a technique for suppressing these parasitic oscillation modes based on index matching the crystal edges with an absorbing doped polymer thermoplastic has recently been developed and demonstrated for large aperture (10 cm in diameter) Ti:sapphire disk amplifiers [115]. The thermoplastic has a refractive index of 1.6849 for 800-nm light and the thus Fresnel reflection at the Ti:sapphire interface is estimated to be ~ 0.048%. According to the model calculation, no parasitic oscillation occurs across the input face of the crystal until the transverse gain is reached to ~ 2100.

Figure 13 (a) shows the calculated transverse gain on the disk faces as a function of the beam diameter. The parasitic oscillation limit (gain ~ 2100) for the crystal edge with the edge cladding is also indicated. According to the calculated result, the beam diameter should be set to be at least ~ 40-mm in order to prevent the parasitic oscillation. The pump fluence is calculated to be ~ 5.6-J/cm^2 at the parasitic oscillation threshold. Figure 13 (b) then shows the calculated results for the achievable output energy depending on the beam diameter. Number of passes of the 800-nm beam is varied from single- to triple-pass configuration and the 800-nm input energy is assumed to be 2.5-J in this calculation. At the diameter of 50-mm, sufficient amplifier efficiencies to produce petawatt pulses would be achieved in the triple-pass configuration. Here, the achievable amplified output energy is estimated to be ~ 40-J in the triple-pass configuration and at the

beam diameter of 50-mm.

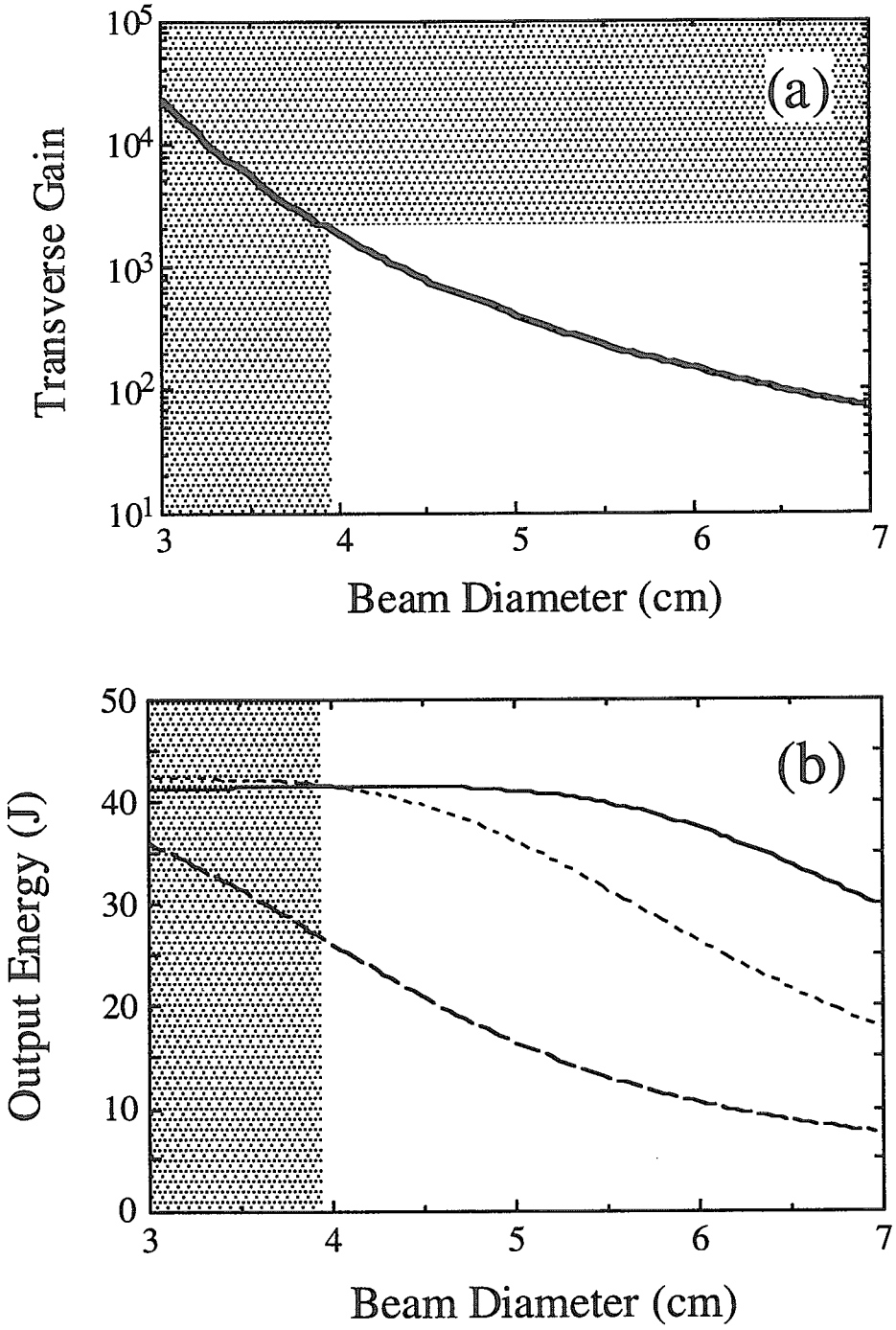

Fig. 13 Calculated results of (a) transverse gain and (b) output energies as a function of the beam diameter for 70 J pump energy. A broken line (single-pass), a doted line (double-pass), and a solid line (triple-pass) represent the calculated output energies. Shaded regions are above parasitic oscillation threshold.

A plan is also in place to develop a repetitive (> 1-Hz) petawatt class laser in APRC. Scaling of the system to higher repetition rates is primarily limited by the availability of suitable pump lasers. Dane et al. have developed a flash lamp pumped Nd:glass zig-zag slab amplifier system with SBS wave-front correction for x-ray generation from laser produced plasmas and other applications [118]. The system produces diffraction-limited output pulses of nearly 30-J with an average output power of 150-W at a 6-Hz repetition rate. Recently this amplifier design has been used to generate spatially and temporally coherent 120-J output pulses from four discrete Nd:glass zig-zag amplifiers [119]. Such systems would be ideal for pumping the large aperture Ti:sapphire disks to produce high-energy pulses with near diffraction-limited beam quality at a few Hz operation. The recent advances in diode-pumped solid-state laser (DPSSL) technology may also become available for pumping of Ti:sapphire. For instance, the Mercury laser which is currently scheduled to be built at LLNL is designed to produce 100-J, 10-Hz pulses by diode pumping Yb:S-FAP. 1047-nm output with an overall electrical efficiency of ~ 10% is predicted [120, 121]. This technology should allow the development of more efficient, compact and high-repetition-rate petawatt Ti:sapphire lasers in the near future.

4. 2 OPTIMIZATION OF AN AMPLIFIED SPECTRUM

We have developed a model for the CPA including the effects of regenerative pulse shaping, gain narrowing, and gain saturation, in which we adapted a frequency-dependent emission cross section to consider gain narrowing as well as a temporally varying population inversion to take into account gain saturation in Ti:sapphire [91]. By using this model, we have performed the simulation of the booster amplifier in order to obtain the largest bandwidth of the amplified pulse, while simultaneously extracting as much energy as possible. Calculated power spectra for four different amplifiers are shown in Fig. 14. These amplifiers are pumped by 50-mJ, 700-mJ, 6.5-J, and 70-J of 532-nm radiation, respectively, in order of their positions in the amplifier chain. Two solid etalons (thickness of 2.0-μm and 1.9-μm) are used for regenerative pulse shaping in the Ti:sapphire regenerative amplifier. In this calculation, the incidence angles of two etalons are set to be 18° and 33°, respectively. The spectral width and energy of the amplified pulse at the output of the booster amplifier are ~ 75-nm and ~ 40-J, respectively. Thus the amplified spectrum can support a transform limited pulse duration of 22-fs.

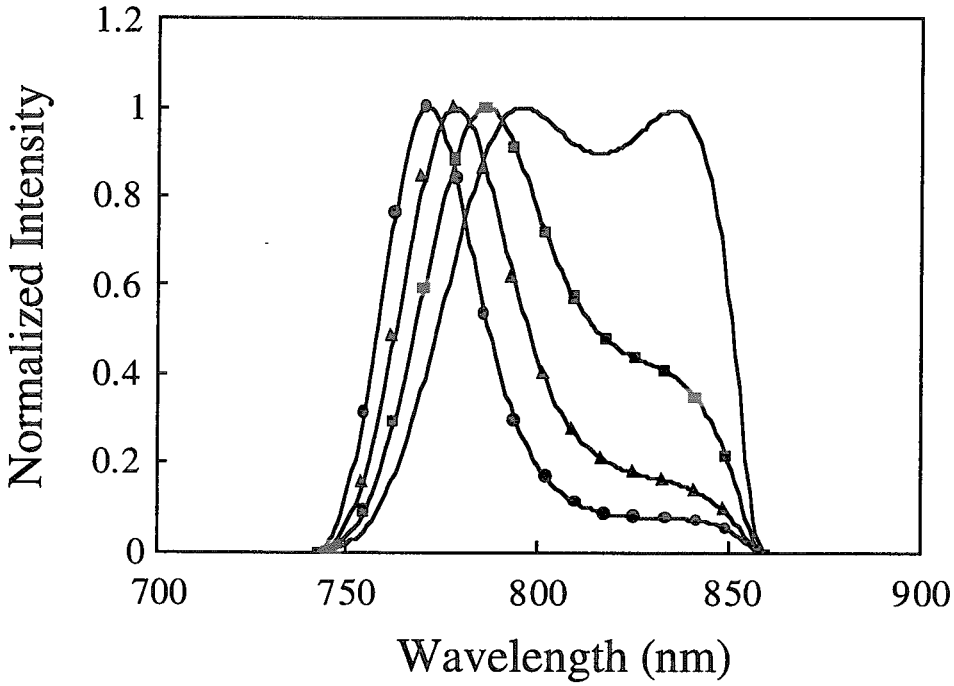

Fig. 14 Calculated spectra after a regenerative amplifier (circles), a four-pass preamplifier (triangles), a four-pass power amplifier (squares) and a three-pass booster amplifier (solid curve). Two solid etalons are used for regenerative pulse shaping.

4．3 HIGH-ORDER-DISPERSION COMPENSATION

As we mentioned in Section II, several groups have demonstrated dispersive optical systems which are capable of controlling dispersion up to fourth order [78-81]. We have designed a mixed grating expander/compressor [81] which consists of the Offner triplet expander [122] and Tracy-type compressor [43] for the petawatt-class laser pulse compression. In order to compensate for the phase distortion of the material in the laser chain, we have chosen a 1200-groove/mm ruled grating in the expander and 1480-groove/mm holographic gratings in the compressor. Diffraction efficiencies of the compressor gratings are critical in terms of the available output pulse energy after compression in CPA systems. The diffraction efficiency of the compressor gratings has been reported to be higher for 1480-groove/mm holographics gratings than for 1200-groove/mmruled gratings, thus the overall efficiency of the compressor should be greater. [123]. In addition, the size of ruled gratings is limited by the size of the initial master grating, which is typically of order 30 cm. Holographic gratings of meter diameter have been recently manufactured and shown to be capable of supporting pulses with energies of

100's of joules [62].

Table I The phase distortions for a Offner triplet expander /112 cm of BK7/ Tracy-type compressor combination. A 1200 groove/mm grating in the expander and 1480 groove/mm gratings in the compressor are used.

	Stretcher	Compressor	Materials
GDD (fs^2/radian)	4.412E+06	-4.462E+06	4.95E+04
Cubic (fs^3/radian^2)	-1.907E+07	1.903E+07	3.61E+04
Quartic (fs^4/radian^3)	1.311E+08	-1.310E+08	-1.24E+04
Quintic (fs^5/radian^4)	-1.247E+09	1.254E+09	3.83E+04

The simultaneous compensation of second-, third-, and fourth-order phase dispersion can be realized theoretically by adjustment of three parameters; the incident angle onto the grating, the separation between the gratings, and groove density in the expander and/or compressor. In the expander, the optimized incident angle and perpendicular separation between gratings are 8.5° and 627-mm, respectively. In the compressor, the incident angle and separation are also calculated to be 24.4° and 544-mm, respectively. Under these conditions, the calculated phase dispersions are listed in Table I. In this calculation, BK7 of 112-cm was used as a simulation of the dispersive materials in the whole laser system. Although the fourth-order dispersion compensation can be accomplished here, the residual fifth-order dispersion would broaden the initial 20-fs pulse to 25-fs duration as shown in Fig. 15. This expander design would expand the seed pulse to ~ 800-ps duration for spectral bandwidth of 70-nm. The bandpass of the expander is approximately 100-nm (centered at 800-nm). The sufficiently long duration chirped pulses should also ensure safe operation of the final amplifiers well above the saturation fluence of Ti:sapphire and thus efficient energy extraction.

The compressor will consists of four gold coated 1480-groove/mm holographic gratings in vacuum. A four-grating arrangement is determined by the maximum available size of the 1480-groove/mm gratings and the onset of optical breakdown of the coating material on the last grating. The sizes of the gratings are 220-mm x 165-mm for the first and last gratings and 420-mm x 210-mm for the second and third gratings, respectively. The diffraction efficiency of these gratings was expected to be greater than 92% over the 100-nm bandwidth (centered at 800-nm), and thus the overall efficiency should be greater than 70%. Based on the efficiency of the gratings, the energy of the compressed pulse is

estimated to be > 28-J. Thus, the peak power for laser pulse is expected to be > 1.1-PW.

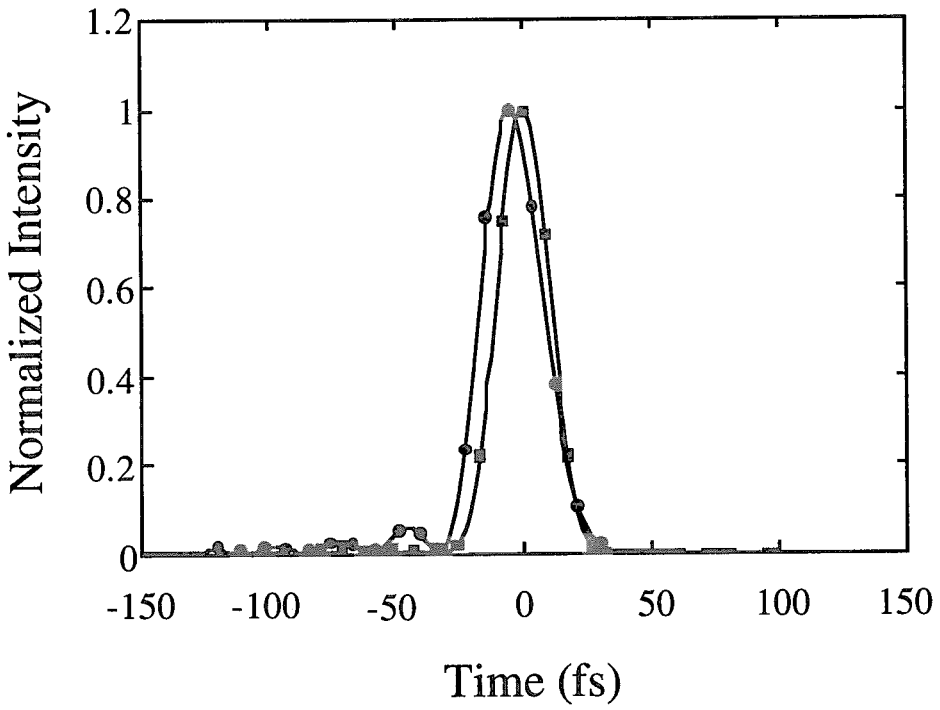

Fig. 15 Output pulse shape (circles) for a 20-fs input pulse (squares) with mixed gratings.

5. APPLICATIONS

Among the numerous possible applications of 100 TW-class, ultrafast laser systems are studies of relativistic laser/matter interactions, laser-generation of high-energy electrons and ions and laser generation and application of coherent and incoherent x-rays. We present here a few of the recent topics proposed and demonstrated by APRC.

5. 1 HIGH-FIELD ATOMIC IONIZATION EXPERIMENTS

In high-field physics experiments, the peak intensity is one of the most important issues for studying light-matter interaction in the relativistic regime. In general, a focused intensity can be estimated by measuring the energy, pulse duration, and spot size of the laser pulse. For example, a Gaussian spatial profile is assumed and the peak intensity is estimated as $0.61E/(\tau \pi r^2)$, where E is the laser energy, τ is the pulse duration (FWHM), and r is the radius of the spot size (half width at half maximum: HWHM). This estimation, however, is uncertain by a factor of 2 - 3, because the full energy in the

experiment is not always concentrated in the central portion of the spatial and temporal profiles. A direct measurement of the peak intensity can be determined from the single atom ionization rate of Ammosov-Delone-Krainov (ADK) theory [124]. Ionization in a strong laser field has been investigated extensively, and for many gases and various wavelengths the intensity dependence of the ion yield has been observed and compared with the calculated dependence. Augst et al. reported experimentally that below 10^{18} W/cm^2 the observed ion-production curves of noble gases agree with curves predicted by ADK theory and barrier suppression ionization [125]. Walker et al. have recently reported observing charge states in argon up to Ar^{16+} which corresponds to a peak intensity of 5×10^{19} W/cm^2 [59].

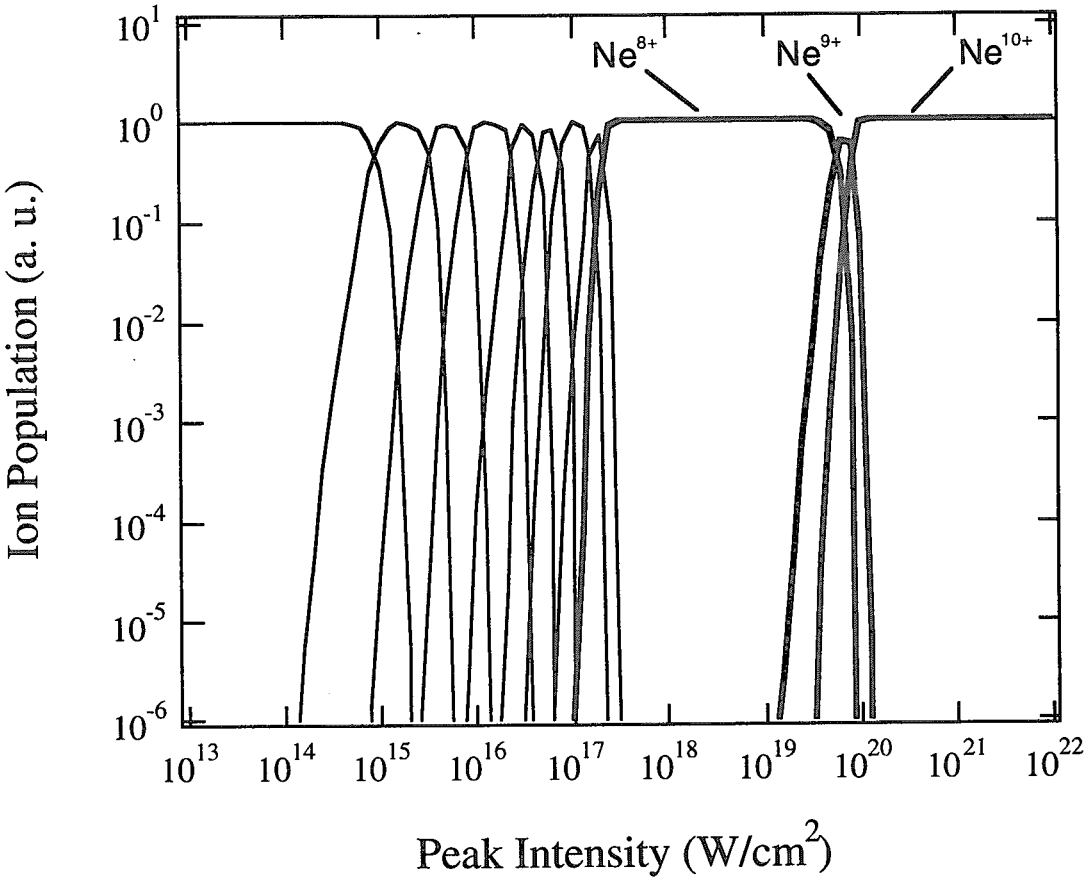

Fig. 16 Calculated ion population of the neon atom as a function of the peak intensity. The thin solid lines represent the populations from neutral neon to Ne^{7+}, and the thick solid lines represent Ne^{8+}, Ne^{9+}, and Ne^{10+}, respectively.

Figure 16 shows the ion population of neon calculated by ADK theory as a function of the peak intensity for pulse duration of 20-fs. From this calculation, Ne^{8+} can be

produced at a peak intensity of 3×10^{17} W/cm^2 defined as $\int W^{ADK} dt = 1$, where W^{ADK} is the ionization rate of ADK theory. Using the peak intensity at which Ne^{8+} occurs as a base, we can characterize the peak intensity well over 10^{18} W/cm^2 from the energy scaling of the laser pulse.

Fully stripped neon ion is generated over 10^{20} W/cm^2 and the maximum charge states of argon, krypton, and xenon correspond to Ar^{16+}, Kr^{26+}, and Xe^{36+} at this peak intensity, respectively. However, comparison of the ion yield with ADK theory has not yet been demonstrated in the ultrahigh-intensity regime ($> 10^{20}$ W/cm^2). Electrons oscillating in such an ultra-intense laser field are relativistic. This makes it possible to investigate an entirely new class of physical effects such as relativistic self-focusing of the laser pulse [126] and harmonic generation by relativistic electrons [127] in an ultrahigh-intensity laser field. In order to clarify the ionization mechanisms of an atom including the ionization rate, the 100 TW Ti:sapphire laser system is currently being applied to perform high-field atomic ionization experiments at 10^{20} W/cm^2.

5. 2 OTHER POTENTIAL APPLICATIONS

Recently, there has been much interest in the generation of coherent [8-14] and incoherent x-rays [4-7, 128], high-energy electrons [27-29] and ions [129] for many applications. X-rays have played a role in helping us understand material structures. In addition to static structural information, transient information is important to the study of the material dynamics. Many of processes such as the breaking and formation of chemical bonds and phase transitions in the materials occur in a few picoseconds or less. Time-resolved x-ray diffraction is the most suitable tool to observe these processes directly at the atomic level [130-135]. Thus, developing ultrafast, high brightness incoherent and coherent laser-based x-ray sources will be of fundamental importance to many dynamic studies in chemistry, biology and physics.

Ueshima et al. have theoretically shown that a relativistically ultrashort laser pulse can produce a large flux of x-rays through the mechanism of Larmor radiation (due to the acceleration of electrons in the strong laser electromagnetic fields) [136]. For example, with the 100-TW laser focused down to 3 μm, 1-keV x-rays are predicted to be emitted with pulse duration on the order of the optical period of the incident laser pulse.

Other more traditional coherent x-ray schemes should also benefit from these new ultrafast CPA laser systems. Inner-shell photoionization x-ray laser schemes were first proposed by Duguay and Rentzepis in 1967 [137]. This simple photoionization x-ray laser, however, has not yet been demonstrated because of the lack of sufficiently fast and

energetic x-ray pump sources. It may be possible for Larmor x-ray radiation to be used as a pump source for such inner-shell ionization x-ray lasers [138].

Laser accelerated electron and ion beams may become useful sources for medical or industrial radiology. The propagation of intense laser pulses in gases and plasmas should be considered for these practical applications [139-144]. Hosokai et al. have recently studied an optical guidance by the implosion phase of a fast Z-pinch discharge in a gas-filled capillary for the channel guided laser wakefield acceleration [145]. They showed that optical guiding of a high-intensity Ti:sapphre laser pulses over a distance of 2-cm, corresponding to 12.5 times the Raylieigh length in an electron density range of 10^{16} – 10^{18} cm^{-3}. Combination of this technique and 100-TW laser pulses could lead to interaction regions sufficient to produce GeV-class electrons.

Nuclear physics may also be brought to the table-top. Yamagiwa and Koga have proposed for the production of ^{18}F via $^{18}O(p, n)^{18}F$ reactions with fast MeV protons from the interaction of a relativistically-intense ultrashort pulse laser with an underdense plasma layer [146]. They have estimated that the yield of ^{18}F could reach $10^{14}S^{-1}$, which is two orders of magnitude larger than from an ordinary cyclotron, thus greatly increasing cost effectiveness of such reactions.

6. CONCLUSION

The ultrafast CPA architectures that have been described in this article open to a new route for the production of the optical pulses with duration on the order of ten femtoseconds to be amplified to multiterawatt peak powers. With a compact three-stage Ti:sapphire CPA system, near diffraction limited and spectrally limited sub-20-fs duration pulses with a peak power in excess of 100-TW have been produced. Since this laser system operates reliably at a 10-Hz repetition rate, it should allow the use sampling and averaging techniques even in the ultrahigh intensity regime ($> 10^{20}$ W/cm^2). Based on design studies which include the suppression of parasitic oscillation across the large-aperture Ti:sapphire amplifier disk, the optimization of the amplified pulse spectrum at the output of the amplifier and the compensation of high-order dispersion in the laser chain with a mixed grating scheme, scaling of 20-fs CPA technology to the petawatt peak power level seems quite feasible. These lasers have opened the door to investigations of entirely new classes of physical effects and applications and should have a major impact on science and technology.

ACKNOWLEDGEMENT

The authors would like to acknowledge encouragement given by T. Arisawa, Y. Kato and H. Ohno.

REFERENCES

[1] G. Mourou, C. P. J. Barty, and M. D. Perry, "Ultrahigh-intensity lasers: physics of the extreme on a tabletop," Phys. Today, vol. 51, pp. 22-28, 1998.

[2] D. Umstadter, S.-Y. Chen, A. Maksimchuk, G. Mourou, and R. Wagner, "Nonlinear Optics in Relativistic Plasmas and Laser Wake Field Acceleration of Electrons," Science vol. 273, pp. 472-475 , 1996.

[3] J. D. Kmetec, C. L. Gordon, III, J. J. Macklin, B. E. Lemoff, G. S. Brown, and S. E. Harris, "MeV x-ray generation with a femtosecond laser," Phys. Rev. Lett., vol.68, pp.1527-1530, 1992.

[4] J. D. Kmetec, "Ultrafast laser generation of hard x-rays," IEEE J. Quantum Electron., vol. QE-28, pp. 2382-2387, 1992.

[5] Z. Jiang, J. C. Kieffer, J. P. Matte, M. Chaker, O. Peyrusse, D. Gilles, G. Korn, A. Maksimchuk, S. Coe, and G. Mourou, "X-ray spectroscopy of hot solid density plasmas produced by subpicosecond high contrast laser pulses at 10^{18}-10^{19} W/cm^2," Phys. Plasma, vol. 2, pp. 1702-1711, 1995.

[6] J. Workman, A. Maksimchuk, X. Liu, U. Ellenberger, J. S. Coe, C. Y. Chien, and D. Umstadter, "Control of bright picosecond X-ray emission from intense subpicosecond laser-plasma interactions," Phys. Rev. Lett., vol. 75, pp. 2324-2327, 1995.

[7] J. F. Pellrtier, M. Chaker, and J. C. Kieffer, "Picosecond soft-x-ray pulses from a high-intensity laser-plasma source," Opt. Lett., vol. 21, pp. 1040-1042, 1996.

[8] A. L'Huillier, and P. Balcou, "High-order harmonic generation in rare gases with a 1-ps 1053-nm laser," Phys. Rev. Lett., vol. 70, pp. 774-777, 1993.

[9] J. J. Macklin, J. D. Kmetec, and C. L. Gordon III, "Higher order harmonic generation using intense femtosecond pulses," Phys. Rev. Lett., vol. 70, pp. 766-769, 1993.

[10] J. Zhou, J. Peatross, M. M. Murnane, and H. C. Kapteyn, "Enhanced high-harmonic generation using 25 fs laser pulses," Phys. Rev. Lett., vol. 76, pp. 752-755, 1996.

[11] C. Spielmann, N. H. Burnett, S. Sartania, R. Koppitsch, M. Schnurer, C. Kan, M. Lenzner, P. Wobrauschek, and F. Krausz, "Generation of coherent X-rays in the water window using 5-fs laser pulses," Science, vol. 278, pp. 661-663, 1997.

[12] M. Schnurer, C. Spielmann, P. Wobrauschek, C. Streli, N. H. Burnett, C. Kan, K. Ferencz, R. Koppitsch, Z. Cheng, and F. Krausz, "Coherent 0.5-keV X-ray emission from helium driven by a sub-10 fs laser," Phys. Rev. Lett., vol. 80, pp. 3236-3238, 1998.

[13] T. Sekikawa, T. Ohno, T. Yamazaki, Y. Nabekawa, and S. Watanabe, "Pulse compression of a high-order harmonic by compensating the atomic dipole phase," Phys. Rev. Lett., vol. 83, pp. 2564-2567, 1999.

[14] Y. Tamaki, J. Itatani, Y. Nagata, M. Obara, and K. Midorikawa, "Highly efficient, phase-matched high-harmonics generation by a self-guided laser beam," Phys. Rev. Lett., vol. 82, pp. 1422-1425, 1999.

[15] P. A. Norreys, M. Zepf, S. Moustaizis, A. P. Fews, J. Zhang, P. Lee, M. Bakarezos, C. N. Danson, A, Dyson, P. Gibbon, P. Loukakos, D. Neely, F. N. Walsh, J. S. Wark, and A. E. Dangor, "Efficient extreme UV harmonics generated from picosecond laser pulse interactions with solid targets," Phys. Rev. Lett., vol. 76, pp. 1832-1835, 1996.

[16] R. Lichters, J. Meyer-ter-Vehn, and A. Pukhov, "Short-pulse laser harmonics from oscillating plasma surfaces driven at relativistic intensity," Phys. Plasmas., vol. 3, pp. 3425-3437, 1996.

[17] P. Gibbon, "High-order harmonic generation in plasmas," IEEE J. Quantum Electron., vol. 33, pp. 1915-1924, 1997.

[18] D. von der Linde, "Generation of high order optical harmonics from solid surfaces", Appl. Phys. B, vol. 68, pp. 315-319, 1999.

[19] H. C. Kapteyn, "Potoionization-pumped x-ray lasers using ultrashort-pulse excitation," Appl. Opt., vol. 31, pp. 4931-4939, 1992.

[20] S. J. Moon and D. C. Eder, "Theoretical investigation of an ultrashort-pulse coherent x-ray source at 45 Å," Phys. Rev. A, vol. 57, pp. 1391-1394, 1998.

[21] N. H. Burnett and P. B. Corkum, "Cold plasma production for recombination extreme ultraviolet lasers by optical field induced ionization," J. Opt. Soc. Am. B, vol. 6, pp. 1195-1199, 1989.

[22] P. Armendt, D. Eder, and S. Wilks, "X-ray lasing by optical-field-induced ionization," Phys. Rev. Lett., vol. 66, pp. 2589-2592, 1991.

[23] Y. Nagata, K. Midorikawa, S. Kubodera, M. Obara, H. Tashiro, and K. Toyoda, "Soft-x-ray amplification of the Lyman-α transition by optical-field-ionization," Phys. Rev. Lett., vol. 71, pp. 3774-3777, 1993.

[24] B. E. Lemoff. G. Y. Yin, C. L. Gordon III, C. P. J. Barty, and S. E. Harris, "Demonstration of a 10-Hz femtosecond-pulse-driven XUV laser at 41.8 nm in Xe IX," Phys. Rev. Lett., vol. 74, pp. 1574-1577, 1995.

[25] T. Tajima and J. M. Dawson, "Laser electron accelerator," Phys. Rev. Lett., vol. 43, pp. 267-270, 1979.

[26] P. Sprangle, E. Esarey, A. Ting, and G. Joyce, "Laser wakefield acceleration and relativisitc optical guiding," Appl. Phys. Lett., vol. 53, pp. 2146-2148, 1988.

[27] K. Nakajima, D. Fisher, T. Kawakubo, H. Nakanishi, A. Ogata, Y. Kato, Y. Kitagawa, R. Kodama, K. Mima, H. Shiraga, K. Suzuki, K. Yamakawa, T. Zhang, Y. Sakawa, T. Shoji, N. Yugami, M. Downer, and T. Tajima, "Observation of ultrahigh gradient electron acceleration by a self-modulated intense short laser pulse," Phys. Rev. Lett., vol. 74, pp. 4428-4431, 1995.

[28] A. Modena, Z. Najmudin, A. E. Dangor, C. E. Clayton, K. A. Marsh, C. Joshi, V. Malka, C. B. Darrow, C. Danson, D. Neely, and F. N. Walsh, "Electron acceleration from the breaking of relativistic plasma waves," Nature, Vol. 377, pp. 606-608, 1995.

[29] R. Wagner, S.–Y. Chen, A. Maksimchuk, and D. Umstadter, "Electron acceleration by a laser wakefield in a relativistically self-guided channel," Phys. Rev. Lett., vol. 78, pp. 3125-3128, 1997.

[30] T. E. Cowan, A. W. Hunt, T. W. Phillips, S. C. Wilks, M. D. Perry, C. Brown, W. Fountain, S. Hatchett, J. Johnson, M. H. Key, T. Parnell. D. M. Pennington, R. A. Snavely, and Y. Takahashi, "Photonuclear fission from high energy electrons from ultraintense laser-solid interactions," Phys. Rev. Lett., vol. 84, pp. 903-906, 2000.

[31] K. W. D. Ledingham, I. Spencer, T. McCanny, R. P. Singhal, M. I. K. Santala, E. Clark, I. Watts, F. N. beg, M. Zepf, K. Krushelnick, M. Tatarakis, A. E. Dangor, P. A. Norreys, R. Allott, D. Neely, R. J. Clark, A. C. Machacek, J. S. Wark, A. J. Cresswell, D. C. W. Sanderson, and J. Magill, "Photonuclear Physics when a multiterawatt laser pulse interacts with solid targets," Phys. Rev. Lett., vol. 84, pp. 899-902, 2000.

[32] R. Sauerbrey, "Acceleration in femtosecond laser-produced plasmas," Phys. Plasmas, vol. 3, pp. 4712-4716, 1996.

[33] H. Takabe, "Laboratory astrophysics with intense and ultra-intense lasers," AIP Conference Proceedings of the International Conference on Superstrong Fields in Plasmas, No.426, pp. 560-570, Edited by: M. Lontano, G. Mourou, F. Pegoraro, and E. Sindoni, AIP Press, 1998.

[34] M. Tabak, J. Hammer, M. E. Glinsky, W. L. Kruer, S. C. Wilks, J. Woodworth, E. M. Campbell, M. D. Perry, and R. J. Mason, "Ignition and high gain with ultrapowerful lasers," Phys. Plasmas, vol. 1, pp. 1626-1634, 1994.

[35] C. Deutsch, H. Furukawa, K. Mima, M. Murakami, and K. Nishihara, "Interaction physics of the fast ignitor concept," Phys. Rev. Lett., vol. 77, pp. 2483-2486, 1996.

[36] D. Strickland and G. Mourou, "Compression of amplified chirped optical pulses," Opt. Commun., vol. 56, pp. 219-221, 1985.

[37] M. D. Perry and G. Mourou, "Terawatt to Petawatt subpicosecond lasers," Science, vol. 64, pp. 917-924, 1994.

[38] J. D. Kmetec, J. J. Macklin and J. F. Young, "0.5-TW, 125-fs Ti:sapphire laser," Opt. Lett., vol. 16, pp. 1001-1003, 1991.

[39] J. P. Chambaret, C. Le Blanc, A. Antonetti, G. Cheriaux, P. F. Curley, G. Darpentigny, and F. Salin, "Generation of 25 TW, 32 fs pulses at 10 Hz," Opt. Lett. vol. 21, pp. 1921-1923, 1996.

[40] C. P. J. Barty, T. Guo, C. Le Blanc, F. Raksi, C. Rose-Petruck, J. Squier, K. R. Wilson, V. V. Yakovlev, and K. Yamakawa, "Generation of 18-fs, multiterawatt pulses by regenerative pulse shaping and chirped-pulse amplification," Opt. Lett., vol. 21, pp. 668-670, 1996.

[41] K. Yamakawa, M. Aoyama, S. Matsuoka, T. Kase, Y. Akahane and H. Takuma, "100-TW, sub-20-fs Ti:sapphire laser system operating at a 10 Hz repetition rate," Opt. Lett., vol. 23, pp. 1468-1470, 1998.

[42] O. E. Martinez, "3000 times grating compressor with positive group velocity dispersion: application to fiber compensation in 1.3 – 1.6 μm region," IEEE J. Quantum Electron., vol. QE-23, pp. 59-64, 1987.

[43] E. B. Treacy, "Optical pulse compression with diffraction gratings," IEEE J. Quantum Electron., vol. 5, pp. 454-458, 1969.

[44] K. Yamakawa, M Aoyama, S. Matsuoka, H. Takuma, C. P. J. Barty and D. Fittinghoff, "Generation of 16 fs, 10 TW pulses at a 10 Hz repetition rate with efficient Ti:sapphire amplifiers," Opt. Lett., vol. 23, pp. 525-527, 1998.

[45] P. Maine, D. Strickland, P. Bado, M. Pessot, and G. Mourou, "Generation of ultrahigh peak power pulses by chirped pulse amplification," IEEE J. Quantum Electron., vol. QE-24, pp. 398-403, 1988.

[46] C. Sauteret, D. Husson, G. Thiell, S. Seznec, G. Gray, A. Migus, and G. Mourou, "Generation of 20-TW pulses of picosecond duration using chirped-pulse amplification in a Nd:glass power chain," Opt. Lett., vol. 16, pp. 238-240, 1991.

[47] F. G. Patterson, R. Gonzales and M. D. Perry, "Compact 10-TW, 800-fs Nd:glass laser," Opt. Lett., vol. 16, pp. 1107-1109, 1991.

[48] K. Yamakawa, H. Shiraga, Y. Kato and C. P. J. Barty, "Prepulse-free 30-TW, 1-ps Nd:glass laser," Opt. Lett., vol. 16, pp. 1593-1595, 1991.

[49] K. Yamakawa, C. P. J. Barty, H. Shiraga and Y. Kato, "Generation of a high-energy picosecond laser pulse with a high-contrast ratio by chirped-pulse amplification," IEEE J. Quantum Electron., vol. QE-27, pp. 288-294, 1991.

[50] C. Rouyer, E. Mazataud, I. Allais, A. Pierre, S. Seznec, C. Sauteret, G. Mourou, and A. Migus, "Generation of 50-TW femtosecond pulses in a Ti:sapphire/Nd:glass chain," Opt. Lett., vol. 18, pp. 214-216, 1993.

[51] B. C. Stuart, M. D. Perry, J. Miller, G. Tietbohl, S. Herman, J. A. Britten, C. Brown, D. Pennington, V. Yanovsky, and K. Wharton, "125-TW Ti:sapphire/Nd:glass laser system," Opt. Lett., vol. 22, pp. 242-244, 1997.

[52] M. Pessot, J. Squier, P. Bado, G. Mourou, and D. J. Harter, "Chirped pulse amplification of 300 fs pulses in an Alexandrite regenerative amplifier," IEEE J. Quantum Electron., vol. QE-25, pp. 61-66, 1989.

[53] M. Pessot, J. Squier, P. Bado, G. Mourou, and D. J. Harter, "Chirped pulse amplification of 100 fs pulses," Opt. Lett., vol. 14, pp. 797-799, 1989.

[54] C. P. J. Barty, C. L. Gordon III, and B. E. Lemoff, "Multiterawatt 30-fs Ti:sapphire laser system," Opt. Lett., vol. 19, pp. 1442-1444, 1994.

[55] J. Zhou, C.-P. Huang, M. M. Murnane, and H. C. Kapteyn, "Amplification of 26-fs, 2-TW pulses near the gain-narrowing limit in Ti:sapphire," Opt. Lett., vol. 20, pp. 64-66, 1995.

[56] A. Sullivan, H. Hamster, H. C. Kapteyn, S. Gordon, W. White, H. Nathel, R. J. Blair, and R. W. Falcone, "Multiterawatt, 100-fs laser," Opt. Lett., vol. 16, pp. 1406-1408, 1991.

[57] A. Sullivan, J. Bonlie, D. F. Price, and W. E. White, "1.1-J, 120-fs laser system based on Nd:glass-pumped Ti:sapphire," Opt. Lett., vol. 21, pp. 603-605, 1996.

[58] K. Yamakawa, A. Magana, P. H. Chiu, and J. D. Kmetec, "Generation of high peak and average power femtosecond pulses at a 10 Hz repetition rate in a titanium-doped sapphire laser," IEEE J. Quantum Electron., vol. QE-30, pp. 2698-2706, 1994.

[59] B. Walker, C. Toth, D. N. Fittinghoff, T. Guo, D.-E. Kim, C. Rose-Petruck, J. A. Squier, K. Yamakawa, K. R. Wilson, and C. P. J. Barty, "A 50-EW/cm^2 Ti:sapphire laser system for studying relativistic light-matter interactions," Opt. Exp., vol. 5, pp. 196-202, 1999.

[60] T. Ditmire and M. D. Perry, "Terawatt Cr:LiSrAlF$_6$ laser system," Opt. Lett., vol. 18, pp. 426-428, 1993.

[61] P. Beaud, M. Richardson, E. J. Miesak, and B. H. T. Chai, "8-TW 90-fs Cr:LiSAF laser," Opt. Lett., vol. 18, pp. 1550-1552, 1993.

[62] M. D. Perry, D. Pennington, B. C. Stuart, G. Tietbohl, J. A. Britten, C. Brown, S. Harman, B. Golick, M. Kartz, J. Miller, H. T. Powell, M. Vergino, and V. Yanovsky, "Petawatt laser pulses," Opt. Lett. Vol. 24, pp. 160-162 , 1999.

[63] K. Yamakawa, H. Sugio, H. Daido, M. Nakatsuka, Y. Kato, and S. Nakai, "1 Hz, 1 ps, terawatt Nd:glass laser," Opt. Commun., vol. 112, pp. 37-42, 1994.

[64] P. F. Moulton, "Spectroscopic and laser characteristics of Ti:Al_2O_3," J. Opt. Soc. Am. B, vol. 3, pp. 125-33, 1986.

[65] S. A. Payne, L. L. Chase, L. K. Smith, W. L. Kway, and H. M. Newkrik, "Laser performance of $LiSrAlF_6:Cr^{3+}$," J. Appl. Phys., vol. 66, pp. 1051-1054, 1989.

[66] D. E. Spence, P. N. Kean, and W. Sibbett, "60-fsec pulse generation from a self-mode-locked Ti:sapphire laser," Opt. Lett., vol. 16, pp. 42-44, 1991.

[67] B. E. Lemoff and C. P. J. Barty, "Generation of high-peak-power 20-fs pulses from a regeneratively initiated, self-mode-locked Ti:sapphire laser," Opt. Lett., vol. 17, pp. 1367-1369, 1992.

[68] M. T. Asaki, C.-P. Huang, D. Garvey, J. Zhou, H. C. Kapteyn, and M. M. Murnane, "Generation of 11-fs pulses from a self-mode-locked Ti:sapphire laser," Opt. Lett., vol. 18, pp. 977-479, 1993.

[69] A. Stingl, Ch. Spielmann, F. Krausz and R. Szipocs, "Generation of 11-fs pulses from a Ti:sapphire laser without the use of prisms," Opt. Lett. vol. 19, pp. 204-206, 1994.

[70] N. H. Rizvi, P. M. W. French, and J. R. Taylor, "Generation of 33-fs pulses from a passively mode-locked Cr^{3+}:$LiSrAlF_6$ laser," Opt. Lett, vol. 17, pp. 1605-1607, 1992.

[71] J. M. Evans, D. E. Spence, W. Sibbett, B. H. T. Chai, and A. Miller, "50-fs pulse generation from a self-mode-locked Cr^{3+}:$LiSrAlF_6$ laser," Opt. Lett., vol. 17, pp. 1447-1449, 1992.

[72] I. T. Sorokina, E. Sorokin, E. Wintner, A. Cassanho, H. P. Jenssen, and R. Szipocs, "Sub-20 fs pulse generation from the mirror dispersion controlled Cr:LiSGaF and Cr:LiSAF lasers," Appl. Phys. B, vol. 65, pp. 245-253, 1997.

[73] U. Morgner, F. X. Kartner, S. H. Cho, Y. Chen, H. A. Haus, J. G. Fujimoto, E. P. Ippen, V. Scheuer, G. Angelow, and T. Tschudi, "Sub-two-cycle pulses from a Kerr-lens mode-locked Ti:sapphire laser," Opt. Lett., vol. 24, pp. 411-413, 1999.

[74] D. H. Sutter, G. Steinmeyer, L. Gallmann, N. Matuschek, F. Morier-Genoud, U. Keller, V. Scheuer, G. Angelow, and T. Tschudi, "Semiconductor saturable-absorber mirror-assisted Kerr-lens mode-locked Ti:sapphire laser producing pulses in the two-cycle regime," Opt. Lett., vol. 24, pp. 631-633, 1999.

[75] S. Sartania, Z. Cheng, M. Lenzner, G. Tempea, C. Spielmann, F. Krausz, and K. Ferencz, "Generation of 0.1-TW 5-fs optical pulses at a 1-kHz repetition rate," Opt. Lett., vol. 22, pp. 1562-1564, 1997.

[76] C. G. Durfee, III, S. Backus, M. M. Murnane, and H. C. Kapteyn, "Design and implementation of a TW-class high-average power laser system," IEEE J. Select. Topics Quantum Electron., vol. 4, pp. 395-406, 1998.

[77] Y. Nabekawa, Y. Kuramoto, T. Togashi, T. Sekikawa, and S. Watanabe, "Generation of 0.66-TW pulses at 1 kHz by a Ti:sapphire laser," Opt. Lett., vol. 23, pp. 1384-1386, 1998.

[78] W. E. White, F. G. Patterson, R. L. Combs, D. F. Price, and R. L. Shepherd, "Compensation of high-order frequency-dependent phase terms in chirped-pulse amplification systems," Opt. Lett., vol. 18, pp. 1343-1345, 1993.

[79] B. E. Lemoff and C. P. J. Barty, Opt. Lett., "Quintic-phase-limited, spatially uniform expansion and recompression of ultrashort pulses," Opt. Lett., vol. 18, pp. 1651-1653, 1993.

[80] S. Kane and J. Squier, "Fourth-order-dispersion limitations of aberration-free chirped pulse amplification systems," J. Opt. Soc. Am. B, vol. 14, pp. 1237-1244, 1997.

[81] J. Squier, C. P. J. Barty, F. Salin, C. Le Blanc, and S. Kane, "Use of mismatched grating pairs in chirped-pulse amplification systems," Appl. Opt., vol. 37, pp. 1638-1641, 1998.

[82] L. M. Frantz and J. S. Nodvik, "Theory of pulse propagation in a laser amplifier," J. Appl. Phys., vol. 34, pp. 2346-2349, 1963.

[83] C. P. J. Barty, G. Korn, F. Raksi, C. Rose-Petruck, J. Squier, A.-C. Tien, K. R. Wilson, V. V. Yakovlev, and K. Yamakawa, "Regenerative pulse shaping and amplification of ultrabroadband optical pulses," Opt. Lett. vol. 21, pp. 219-221, 1996.

[84] K. Yamakawa, T. Guo, G. Korn, C. Le Blanc, F. Raksi, C. Rose-Petruck, J. Squier, K. R. Wilson, V. Yakovlev, and C. P. J. Barty, "Techniques for controlling of gain narrowing during ultrashort pulse amplification," Proceedings of the SPIE, "Generation, Amplification, and Measurement of Ultrashort Laser Pulses III," vol. 2701, pp. 198-208, 1996.

[85] A. Stingl, M. Lenzner, Ch. Spielmann, F. Krausz and R. Szipocs, "Sub-10-fs mirror-dispersion-controlled Ti:sapphire laser," Opt. Lett. vol. 20, pp. 602-604, 1995.

[86] M. Aoyama and K. Yamakawa, "Noise characterization of an all-solid-state mirror-dispersion-controlled 10-fs Ti:sapphire laser," Opt. Commun., vol. 140, pp. 255-258, 1997.

[87] C. W. Siders, E. W. Gaul, M. C. Downer, A. Babine, and A. Stepanov, "Self-starting femtosecond pulse generation from a Ti:sapphire laser synchronously pumped by a

pointing-stabilized mode-locked Nd:YAG laser," Rev. Sci. Instr., vol. 65, pp. 3140-3144, 1994.

[88] F. G. Patterson and M. D. Perry, "Design and performance of a multiterawatt, subpicosecond neodymium:glass laser," J. Opt. Soc. Am. B, vol. 8, pp. 2384-2391, 1991.

[89] N. Blanchot, C. Rouyer, C. Sauteret and A. Migus, "Amplification of sub-100 TW femtosecond pulses by shifted amplifying Nd:glass amplifiers: theory and experiments," Opt. Lett. vol. 20, pp. 395-397, 1995.

[90] J. T. Hunt, J. A. Glaze, W. W. Simmons, and P. A. Renard, "Suppression of self-focusing through low-pass spatial filtering and relay imaging," Appl. Opt., vol. 17, pp. 2053-2057, 1978.

[91] K. Yamakawa, M. Aoyama, S. Matsuoka, H. Takuma, D. N. Fittinghoff, and C. P. J. Barty, "Ultrahigh-peak and high-average power chirped-pulse amplification of sub-20-fs pulses with Ti:sapphire amplifiers," IEEE J. Select. Topics Quantum Electron., vol. 4, pp. 385-394, 1998.

[92] P. B. Corkum, F. Brunel, N. K. Sherman, and T. Srinivasan-Rao, "Thermal response of metals to ultrashort-pulse laser excitation," Phys. Rev. Lett., vol. 61, pp. 2886-2889, 1988.

[93] M. M. Murnane, H. C. Kapteyn, and R. W. Falcone, "High-density plasmas produced by ultrafast laser pulses," Phys. Rev. Lett., vol. 62, pp. 155-158, 1989.

[94] D. F. Price, R. M. More, R. S. Walling, G. Guethlein, R. L. Shepherd, R. E. Stewart, and W. E. White, "Absorption of ultrafast laser pulses by solid targets heated rapidly to temperatures 1 – 1000 eV," Phys. Rev. Lett., vol. 75, pp. 252-255, 1995.

[95] D. J. Kane and R. Trebino, "Single-shot measurement of the intensity and phase of an arbitrary ultrashort pulse by using frequency-resolved optical gating," Opt. Lett., vol. 18, pp. 823-825, 1993.

[96] K. W. DeLong, R. Trebino, J. Hunter, and W. E. White, "Frequency-resolved optical gating with the use of second-harmonic generation," J. Opt. Soc. Amer. B, vol. 11, pp. 2206-2215, 1994.

[97] R. Trebino, K. W. DeLong, D. N. Fittinghoff, J. N. Sweetser, M. A. Krumbugel, B. A. Richman, and D. J. Kane, "Measuring ultrashort laser pulses in the time-frequency domain using frequency-resolved optical gating," Rev. Sci. Instrum., vol. 68, pp. 3277-3295, 1997.

[98] A. Baltuska, M. S. Pshenichnikov, and D. A. Wiersma, "Amplitude and phase characterization of 4.5-fs pulses by frequency-resolved optical gating," Opt. Lett., vol. 23, pp. 1474-1476, 1998.

[99] G. Albrecht, A. Antonetti, and G. Mourou, "Temporal shape analysis of Nd^{3+}:YAG active passive mode-locked pulses," Opt. Commun., vol. 40, pp. 59-62, 1981.

[100] D. N. Fittinghoff, B. C. Walker, J. A. Squier, C. S. Toth, C. Rose-Petruck, and C. P. J. Barty, "Dispersion considerations in ultrafast CPA systems," IEEE J. Select. Topics Quantum Electron., vol. 4, pp. 430-440, 1998.

[101] V. Bagnoud and F. Salin, "Global optimization of pulse compression in chirped pulse amplification," IEEE J. Select. Topics Quantum Electron., vol. 4, pp. 445-448, 1998.

[102] E. Zeek, K. Maginnis, S. Backus, U. Russek, M. Murnane, G. Mourou, H. Kapteyn, and G. Vdovin, "Pulse compression by use of deformable mirrors," Opt. Lett., vol. 24, pp. 493-495, 1999.

[103] J. Itatani, J. Faure, M. Nantel, G. Mourou, and S. Watanabe, "Suppression of the amplified spontaneous emission in chirped-pulse-amplification lasers by clean high-energy seed-pulse injection," Opt. Commun., vol. 148, pp. 70-74, 1998.

[104] D. Malacara, ed., *Optical Shop Testing*, 2nd ed. (John Wiley and Sons, New York, 1992) Chap. 10.

[105] D. Malacara, ed., *Optical Shop Testing*, 2nd ed. (John Wiley and Sons, New York, 1992) Chap. 4.

[106] J. Primot and L. Sogno, "Achromatic three-wave (or more) lateral shearing interferometer," J. Opt. Soc. Am. A, vol. 12, pp. 2679-2685 , 1995.

[107] J.-C. Chanteloup, F. Druon, M. Nantel, A. Maksimchuk, and G. Mourou, "Single-shot wave-front measurements of high-intensity ultrashort pulses with a three-wave interferometer," Opt. Lett. vol. 23, pp. 621-623 , 1998.

[108] S. Matsuoka and K. Yamakawa, "Wave-front measurements of terawatt-class ultrashort laser pulses by the Fresnel phase-retrieval method.," J. Opt. Soc. Am. B, vol. 17, pp. 663-667, 2000.

[109] R. W. Gerchberg and W. O. Saxton, "A practical algorithm for the determination of phase from image and diffraction plane pictures," Optik vol. 35, pp. 237-246 , 1972.

[110] J. R. Fienup and C. C. Wackerman, "Reconstruction of an object from the modulus of its Fourier transform," Opt. Lett., vol. 3, pp. 27-29, 1978.

[111] J. R. Fienup, "Phase retrieval algorithms: a comparison," Appl. Opt. Vol. 21, pp. 2758-2769 , 1982.

[112] J. R. Fienup, "Phase-retrieval algorithms for a complicated optical system," Appl. Opt., vol. 32, pp. 1737-1746 , 1993.

[113] J. R. Fienup, J. C. Marron, T. J. Schulz, and J. H. Seldin, "Hubble Space Telescope characterized by using phase-retrieval algorithms," Appl. Opt., vol. 32, pp. 1747-1766 , 1993.

[114] J. W. Goodman, *Introduction of Fourier Optics*, 2nd ed. (McGraw-Hill, New York, 1996).

[115] F. G. Patterson, J. Bonlie, D. Price, and B. White, Suppression of parasitic lasing in large-aperture Ti:sapphire laser amplifiers, Opt. Lett. Vol. 24, pp. 963-965, 1999.

[116] J. M. McMahon, J. L. Emmett, J. F. Holzrichter, and J. B. Trenholme, "A glass-disk-laser amplifier," IEEE J. Quantum Electron. Vol. QE-9, pp. 992-999, 1973.

[117] G. J. Linford, R. A. Saroyan, J. B. Trenholme, and M. J. Weber, "Meaurements and modeling of gain coefficients for neodymium laser glasses," IEEE J. Quantum Electron. Vol. QE-15, pp. 510-523, 1979.

[118] C. B. Dane, L. E. Zapata, W. A. Neuman, M. A. Norton, and L. A. Hackel, "Design and operation of a 150 W near diffraction-limited laser amplifier with SBS wave-front correction," IEEE J. Quantum Electron., vol. QE-31, pp. 148-163, 1995.

[119] C. B. Dane, J. D. Wintemute, B. Bhachu, and L. A. Hackel, "Diffraction-limited, high average power phase-locking of four 30 J beams from discrete Nd:glass zig-zag amplifiers," Conference on Lasers and Electro-Optics, Baltimore MD, May 1997, postdeadline paper CPD.

[120] C. Marshall, L. K. Smith, R. J. Beach, M. A. Emanuel, K. Shaffers, J. Skidmore, S. A. Payne, and B. H. T. Chai, "Diode-pumped ytteribium-doped $Sr_5(PO_4)_3F$ laser Performance," IEEE J. Quantum Electron., vol. QE-32, pp. 650-656, 1996.

[121] C. Orth, R. Beach, C. Bibeau, E. Honea, K, Jancaitis, J. Lawson, C. Marshall, R. Sacks, K. Shaffers, J. Skidmore, and S. Sutton, "Design modeling of the 100-J diode-pumped solid-state laser for project Mercury," SPIE International Symposium on High-Power Laser and Applications, San Jose, CA, January 24-30, 1998. (unpublished)

[122] G. Chériaux, P. Rousseau, F. Salin, J. P. Chambaret, B. Walker, and L. F. Dimauro, "Aberration free expander design for ultrashort-pulse amplification," Opt. Lett. Vol. 21, pp. 414-416, 1996.

[123] R. D. Boyd, J. A. Britten, D. E. Decker, B. W. Shore, B. C. Stuart, and M. D. Perry, "High-efficiency metallic diffraction gratings for laser applications," Appl. Opt., vol. 34, pp. 1697-1706, 1995.

[124] M. V. Ammosov, N. B. Delone, and V. P. Krainov, "Tunnel ionization of complex atoms and of atomic ions in an alternating electromagnetic field," Zh. Eksp. Teor. Fiz., vol. 91, pp. 2008-2013, 1986. [Sov. Phys. JETP, vol. 64, pp. 1191-1194, 1986.]

[125] S. Augst, D. D. Meyerhofer, D. Strickland, and S. L. Chin, "Laser ionization of noble gases by Coulomb-barrier suppression," J. Opt. Soc. Amer. B, vol. 8, pp. 858-867, 1991.

[126] C. Max, J. Arons, and A. Langdon, "Self-modulation and self-focusing of electromagnetic waves in plasmas," Phy. Rev. Lett., vol. 33, pp. 209-212, 1974.

[127] E. Sarachik and G. Schappert, "Classical theory of the scattering of intense laser radiation by free electrons," Phy. Rev. D, vol. 1, pp. 2738-2753, 1970.

[128] A. Rousse, P. Audebert, J. P. Geindre, F. Fallies, J.-C. Gauthier, A. Mysyrowicz, G, Grillon, and A. Antonetti, "Efficient K alpha X-ray source from femtosecond laser-produced," Phys. Rev. E, vol. 50, pp. 2200-2207, 1994.

[129] T. Ditmire, J. W. G. Tisch, E. Springate, M. B. Mason, N. Hay, R. A. Smith, J. Marangos, and M. H. R. Hutchinson, "High-energy ions produced in explosions of superheated atomic clusters," Nature, vol. 386, pp. 54-56, 1997.

[130] C. Rischel, A. Rousse, I. Uschmann, P.-A. Albouy, J.-P. Geindre, P. Audebert, J.-C. Gauthier, E. Forster, J.-L. Martin, and A. Antonetti, "Femtosecond time-resolved X-ray diffraction from laser-heated organic films," Nature, vol. 390, pp. 490-492, 1997.

[131] T. Guo, C. Rose-Petruck, R. Jimenez, F. Raksi, J. Squier, B. Walker, K. R. Wilson, and C. P. J. Barty, "Picosecond-milliangstrom resolution dynamics by ultrafast x-ray diffraction," SPIE. Vol. 3157, pp. 84-90, 1997.

[132] C. Rose-Petruck, R. Jimenez, T. Guo, A. Cavalleri, C. W. Siders, F. Raksi, J. A. Squier, B. C. Walker, K. R. Wilson, and C. P. J. Barty, "Picosecond-milliangstrom lattice dynamics measured by ultrafast X-ray diffraction," Nature, vol. 398, pp. 310-312, 1999.

[133] C. W. Siders, A. Cavalleri, K. Sokolowski-Tinten, C. Toth, T. Guo, M. Kammler, M. Horn von Hoegen, K. R. Wilson, D. von der Linde, and C. P. J. Barty, "Detection of nonthermal melting by ultrafast X-ray diffraction," Science, vol. 286, pp. 1340-1342, 1999.

[134] A. H. Chin, R. W. Schoenlein, T. E. Glover, P. Balling, W. P. Leemans, and C. V. Shank, "Ultrafast structural dynamics in InSb probed by time-resolved x-ray diffraction," Phys. Rev. Lett., vol. 83, pp. 336-339, 1999.

[135] A. M. Lindenberg, I. Kang, S. L. Johnson, T. Missalla, P. A. Heimann, Z. Chang, J. Larsson, P. H. Bucksbaum, H. C. Kapteyn, H. A. Padmore, R. W. Lee, J. S. Wark, and R. W. Falcone, "Time-resolved x-ray diffraction from coherent phonons during a laser-induced phase transition," Phys. Rev. Lett., vol. 84, pp. 111-114, 2000.

[136] Y. Ueshima, Y. Kishimoto, A. Sasaki, and T. Tajima, "Laser Larmor X-ray radiation from low-Z matter," Laser and Particle Beams, vol. 17, pp. 45-58, 1999.

[137] M. A. Duguay and P. M. Rentzepis, "Some approaches to vacuum UV and x-ray lasers," Appl. Phys. Lett., vol. 10, pp. 350-352, 1967.

[138] K. Moribayashi, A. Sasaki, and T. Tajima, "Ultrafast x-ray processes with hollow atoms," Phys. Rev. A, vol. 58, pp. 111-114, 2000.

[139] A. B. Borisov, A. V. Borovskiy, V. V. Korobkin, A. M. Prokhorov, O. B. Shiryaev, X. M. shi, T. S. Luk, A. McPherson, J. C. Solem, K. Boyer, and C. K. Rhodes, "Observation of relativistic and charge-displacement self-channeling of intense subpicosecond ultraviolet (248 nm) radiation in plasmas," Phys. Rev. Lett., vol. 68, pp. 2309-2312, 1992.

[140] A. Sullivan, H. Hamster, S. P. Gordan, R. W. Falcone, and H. Nathel, "Propagation of intense, ultrashort laser pulses in plasmas," Opt. Lett., vol. 19, pp. 1544-1546, 1994.

[141] P. Monot, T. Auguste, P. Gibbon, F. Jakober, G. Mainfray, A. Dulieu, M. Louis-Jacquet, G. Malka, and J. L. Miquel, "Experimental demonstration of relativistic self-channeling of a multiterawatt laser pulse in an underdense plasma," Phys. Rev. Lett., vol. 74, pp. 2953-2957, 1995.

[142] C. G. Durfee, III, and H. M. Milchberg, "Light pipe for high intensity laser pulses," Phys. Rev. Lett., vol. 71, pp. 2409-2411, 1993.

[143] H. M. Milchberg, T. R. Clark, C. G. Durfee, III, T. M. Antonsen, and P. Mora, "Development and applications of a plasma waveguide for intense laser pulses," Phys. Plasmas, vol. 3, pp. 2149-2155, 1996.

[144] A. Zigler, Y. Ehrlich, C. Cohen, J. Krall, and P. Sprangle, "Optical guiding of high intensity laser pulses in a long plasma channel formed by a slow capillary discharge," J. Opt. Soc. Amer. B., vol. 13, pp. 68-71, 1996.

[145] T. Hosokai, M. Kando, H. Dewa, H. Kotaki, S. Kondo, N. Hasegawa, K. Nakajima, and K. Horioka, "Optical guidance of terawatt laser pulses by the implosion phase of a fast Z-pinch discharge in a gas-filled capillary," Opt. Lett., vol. 25, pp. 10-12, 2000.

[146] M. Yamagiwa and J. Koga, "MeV ion generation by an ultra-intense short-pulse laser: application to positron emitting radionuclide production," J. Phys. D: Appl. Phys., vol. 32, pp. 2526-2528, 1999.

This is a blank page.

国際単位系（SI）と換算表

表1　SI基本単位および補助単位

量	名称	記号
長さ	メートル	m
質量	キログラム	kg
時間	秒	s
電流	アンペア	A
熱力学温度	ケルビン	K
物質量	モル	mol
光度	カンデラ	cd
平面角	ラジアン	rad
立体角	ステラジアン	sr

表2　SIと併用される単位

名称	記号
分，時，日	min, h, d
度，分，秒	°, ′, ″
リットル	l, L
トン	t
電子ボルト	eV
原子質量単位	u

1 eV=1.60218×10^{-19}J

1 u=1.66054×10^{-27}kg

表3　固有の名称をもつSI組立単位

量	名称	記号	他のSI単位による表現
周波数	ヘルツ	Hz	s^{-1}
力	ニュートン	N	m·kg/s^2
圧力，応力	パスカル	Pa	N/m^2
エネルギー,仕事,熱量	ジュール	J	N·m
工率，放射束	ワット	W	J/s
電気量，電荷	クーロン	C	A·s
電位，電圧，起電力	ボルト	V	W/A
静電容量	ファラド	F	C/V
電気抵抗	オーム	Ω	V/A
コンダクタンス	ジーメンス	S	A/V
磁束	ウェーバ	Wb	V·s
磁束密度	テスラ	T	Wb/m^2
インダクタンス	ヘンリー	H	Wb/A
セルシウス温度	セルシウス度	℃	
光束	ルーメン	lm	cd·sr
照度	ルクス	lx	lm/m^2
放射能	ベクレル	Bq	s^{-1}
吸収線量	グレイ	Gy	J/kg
線量等量	シーベルト	Sv	J/kg

表4　SIと共に暫定的に維持される単位

名称	記号
オングストローム	Å
バーン	b
バール	bar
ガル	Gal
キュリー	Ci
レントゲン	R
ラド	rad
レム	rem

1 Å=0.1nm=10^{-10}m

1 b=100fm^2=10^{-28}m^2

1 bar=0.1MPa=10^{5}Pa

1 Gal=1cm/s^2=10^{-2}m/s^2

1 Ci=3.7×10^{10}Bq

1 R=2.58×10^{-4}C/kg

1 rad=1cGy=10^{-2}Gy

1 rem=1cSv=10^{-2}Sv

表5　SI接頭語

倍数	接頭語	記号
10^{18}	エクサ	E
10^{15}	ペタ	P
10^{12}	テラ	T
10^{9}	ギガ	G
10^{6}	メガ	M
10^{3}	キロ	k
10^{2}	ヘクト	h
10^{1}	デカ	da
10^{-1}	デシ	d
10^{-2}	センチ	c
10^{-3}	ミリ	m
10^{-6}	マイクロ	μ
10^{-9}	ナノ	n
10^{-12}	ピコ	p
10^{-15}	フェムト	f
10^{-18}	アト	a

(注)

1．表1－5は「国際単位系」第5版，国際度量衡局1985年刊行による。ただし，1 eVおよび1 uの値はCODATAの1986年推奨値によった。

2．表4には海里，ノット，アール，ヘクタールも含まれているが日常の単位なのでここでは省略した。

3．barは，JISでは流体の圧力を表わす場合に限り表2のカテゴリーに分類されている。

4．EC閣僚理事会指令ではbar，barnおよび「血圧の単位」mmHgを表2のカテゴリーに入れている。

換算表

力	N(=10^{5}dyn)	kgf	lbf
	1	0.101972	0.224809
	9.80665	1	2.20462
	4.44822	0.453592	1

粘度　1 Pa·s(N·s/m^2)=10 P(ポアズ)(g/(cm·s))

動粘度　1m^2/s=10^{4}St(ストークス)(cm^2/s)

圧力	MPa(=10bar)	kgf/cm^2	atm	mmHg(Torr)	lbf/in^2(psi)
	1	10.1972	9.86923	7.50062×10^3	145.038
	0.0980665	1	0.967841	735.559	14.2233
	0.101325	1.03323	1	760	14.6959
	1.33322×10^{-4}	1.35951×10^{-3}	1.31579×10^{-3}	1	1.93368×10^{-2}
	6.89476×10^{-3}	7.03070×10^{-2}	6.80460×10^{-2}	51.7149	1

エネルギー・仕事・熱量	J(=10^7 erg)	kgf·m	kW·h	cal(計量法)	Btu	ft·lbf	eV
	1	0.101972	2.77778×10^{-7}	0.238889	9.47813×10^{-4}	0.737562	6.24150×10^{18}
	9.80665	1	2.72407×10^{-6}	2.34270	9.29487×10^{-3}	7.23301	6.12082×10^{19}
	3.6×10^6	3.67098×10^5	1	8.59999×10^5	3412.13	2.65522×10^6	2.24694×10^{25}
	4.18605	0.426858	1.16279×10^{-6}	1	3.96759×10^{-3}	3.08747	2.61272×10^{19}
	1055.06	107.586	2.93072×10^{-4}	252.042	1	778.172	6.58515×10^{21}
	1.35582	0.138255	3.76616×10^{-7}	0.323890	1.28506×10^{-3}	1	8.46233×10^{18}
	1.60218×10^{-19}	1.63377×10^{-20}	4.45050×10^{-26}	3.82743×10^{-20}	1.51857×10^{-22}	1.18171×10^{-19}	1

1 cal= 4.18605J（計量法）

= 4.184J（熱化学）

= 4.1855J（15℃）

= 4.1868J（国際蒸気表

仕事率　1 PS(仏馬力)

= 75 kgf·m/s

= 735.499W

放射能	Bq	Ci
	1	2.70270×10^{-11}
	3.7×10^{10}	1

吸収線量	Gy	rad
	1	100
	0.01	1

照射線量	C/kg	R
	1	3876
	2.58×10^{-4}	1

線量当量	Sv	rem
	1	100
	0.01	1

(86年12月26日現在)